F 4 Electron Theory of Molecular Magnets

A. V. Postnikov
Institut für Festkörperforschung
Forschungszentrum Jülich GmbH

Contents

1 Introduction

Molecular magnets are purely organic or metalloorganic materials, which possess, even in the absence of external magnetic field, stable magnetic moments associated with certain chemical building blocks. Such moments may reside on transition metal ions, or on organic free radicals. Quite often the building blocks, i.e. single molecule magnets (SMM), are chemically stable and maintain their magnetic moments both in a liquid solution and in solid phase. The solidification may result either in molecular crystals, where the SMM are spatially well separated and loosely magnetically bonded, or in polymers, one-, two- or three-dimensionally connected magnetic structures. In broad sense, all there chemical species are sometimes referred to as molecular magnets. More strictly speaking, one tends to narrow this definition to SMM, or to molecular crystals constructed of them. For chemists, metalloorganic compounds with magnetic ions, as well as organic molecules containing free organic radicals, are not basically new materials. Yet, last decades brought about a dramatic increase in the number of synthesized molecular magnets, and considerable progress of their characterization by methods well established in the materials science – Mössbauer spectroscopy, nuclear and electron spin resonance, optical and X-ray spectroscopy. In 1980 Lis [1] reported the synthesis of $Mn_{12}O_{12}(CH_3COO)_{16}(H_2O)_4$, known as Mn_{12}-acetate (Mn_{12}-ac in the following), by now probably the most studied molecular magnet. Its structure is shown in Fig. 1.

The reason why molecular magnets got so much attention in the last decades is that certain interesting physical effects have been found in these systems, specific for molecular magnets and not to conventional magnetic materials. These are effects of purely quantum nature, like single-molecule hysteresis or quantum tunnelling of magnetization . In short, this is about the formation of the resulting spin of a molecule from the spins of participating magnetic atoms, and how the state of the resulting spin can be influenced by external magnetic field. Effects which provide a direct experimental manifestation of quantum mechanics are known to be difficult to detect. In molecular magnets their detection became possible because the systems of study, crystallized SMM, were all identical. Moreover, even as the orchestrated behaviour of

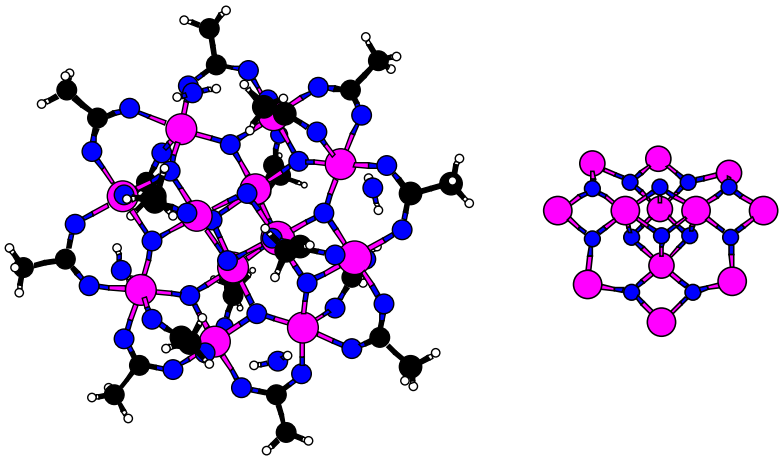

Fig. 1: *Two views of the Mn_{12}-ac. Left panel: the entire molecule, right panel: the magnetic core $Mn_{12}O_{12}$. The eight outer Mn ions have spins $s = 2$ ordered in parallel, the four inner $s = 3/2$ are antiparallel to them; the resulting ferrimagnetic structure has total spin $S = 10$.*

spins occur only below certain temperature, it is in some cases high enough (several K) to be accessible in the lab. There are lectures at this school specifically devoted to quantum theory of molecular magnetism (by J. Schnack) and to quantum tunnelling of magnetization in molecular magnets (by W. Wernsdorfer), which give more details on experimental situation and on the peculiarities of quantum behaviour. Among the review literature for the introduction into the field, one shouldn't miss the monograph by Kahn [2] published in 1993. New chemical species and observed effects since then were subject to many subsequent books, e.g., that edited by Linert and Verdaguer [3], to name a relatively new one. Together with Mark Pederson and Jens Kortus, the author prepared an internet review on the subject [4], an enlarged version of which, updated jointly with Jens Kortus, will be published soon as a book chapter [5]. Some material from the latter publication have been used in preparing the present lecture.

New physics of molecular magnets feeds hopes of certain prospective applications, and such hopes pose the problem of understanding, improving, or predicting desirable characteristics of these materials. The applications which come into discussion are, for instance, magnetic storage (one molecule would store one bit, with much higher information storage density than accessible with microdomains of present-day storage media or magnetic nanoparticles of next future). In order to make this feasible, one needs to make sure that the resulting spin of molecule is formed from constituent atomic spins only in a certain way. That means, the coupling between spins must be strong enough so that thermal fluctuations won't disorganize them. Moreover, the resulting spin must remain stick to a definite orientation relatively to the axes of molecule, and not freely rotate at the effect of temperature. This implies high magnetic anisotropy . These two parameters, strong interatomic magnetic coupling and high magnetocrystalline anisotropy, are therefore desirable for magnetic storage applications. Presently achieved numbers for known molecular magnets (of the order of tens of K) fall far short of desirable values. Other applications, like switching magnetic state of a molecule by light, seem more close. All these applications under discussion deal with the switching between different metastable states of the electron system in the magnetic molecule in question. Therefore it is essential to provide an adequate description of electron characteristics, and understand what they depend upon. This is the subject of the present lecture to show how such description can be achieved, what are the characteristics to look for, and how reliable the obtained results are. It is good to realize that the calculation output, even if obtained by quite reliable methods, must be whenever possible checked against experimental data, for the sake of mutual verification. On the other side, quantum theories of magnetism (the subject of the lecture by J. Schnack), even as they heavily depend on *ad hoc* parametrisation, go well beyond quantitative simulations of electronic structure in what regards the issues of statistical physics and thermodynamics. Therefore the cross-checking between different branches of theory is as equally important.

2 Relevant physical properties and *ab initio* point of view

2.1 Spin Hamiltonians

A comforting feature of modern studies on molecular magnets is that different groups of researchers, be they chemists, experimental physicists, model or ab-initio theorists, employ essentially the same language for representing their results, that is, the language of model Hamiltonians. Consequently, if one agrees on a basic model of underlying physics, one can discuss specific numbers of parameters entering such models, estimated either from experiment, or

from first-principles calculations. This helps to understand whether theory agrees with experiment, and also to verify whether the accepted model was satisfactory, in the first place, or needs revision.

An essential element of such model Hamiltonians are spin operators, that's why we'll speak in the following of spin Hamiltonians. The values of spins of individual atoms which build a particular SMM are usually clear from very basic chemical considerations, such as formal valency; if this is not the case, quite straightforward experimental tools, like magnetization or Mössbauer effect measurements, might provide additional hints. Usually the values of constituent spins are not subject to controversy between experiment and theory; the mechanisms and parameters governing their interaction, on the contrary, often are. In fact the model spin Hamiltonians neglect the true chemical environment and bonding and reduce all interactions to just a few model parameters. One is dependent on experimental input in order to estimate these parameters, and the accuracy of quantitative predictions depends on the parameters chosen. Even more problematic, it is not *a priori* clear which interactions are important and should be included in the model and which are negligible.

Let me now become more specific. The parameterization of a magnetic interaction normally includes, as the presumably leading term, the Heisenberg Hamiltonian

$$\mathcal{H} = -2 \sum_{i>j} J_{ij} \mathbf{S}_i \mathbf{S}_j \,, \tag{1}$$

with the summation indicating that each pair of spins $\mathbf{S}_i$, $\mathbf{S}_j$ is counted only once.[1] As only the relative orientation of both spins matters, this interaction is isotropic.

The dependence on absolute spin orientation, i.e. with respect to the crystal lattice, can be brought in via a modification of the Heisenberg model taking into account anisotropy:

$$\mathcal{H} = -2 \sum_{i>j} J_{ij} \left[S_i^z S_j^z + \gamma (S_i^x S_j^x + S_i^y S_j^y) \right] \,. \tag{2}$$

This form of interaction recovers the conventional Heisenberg model in case of γ=1, reduces to the Ising model for γ=0, or to the 2-dimensional interaction for $\gamma \gg 1$. Surprisingly, even in case of the seemingly simple Ising model so far analytic solutions are known only for one-dimensional and two-dimensional lattices [6].

Further on, the single-spin anisotropy can be included, and the Zeeman term added, yielding

$$\mathcal{H} = -2 \sum_{i>j} J_{ij} (\mathbf{S}_i \mathbf{S}_j) + D \sum_i (\mathbf{e}_i \mathbf{S}_i)^2 + g \mu_{\mathrm{B}} \sum_i \mathbf{B}\, \mathbf{S}_i \,, \tag{3}$$

with the Landé g-factor being normally close to 2, and μ_{B} being the Bohr magneton. The single-spin anisotropy term may lack some of the true physics. It is scaled with its corresponding constant D and depends on the orientation of each spin $\mathbf{S}_i$ relative to a reasonably chosen fixed direction in space $\mathbf{e}_i$; the Zeeman term scales with the external magnetic field B, for the chosen value of the g factor.

Such model spin Hamiltonian can be further sophisticated by introducing additional parameters, i.e., distinguishing between random (varying from site to site) and constant (global) magnetic anisotropy, yielding the appearance of distinct D parameters in Eq. (3). Moreover, higher-order terms in isotropic interaction (biquadratic exchange, etc.), as well as from antisymmetric

[1] Note that the definition of sign and prefactor may vary between publications.

Dzyaloshinsky-Moriya spin exchange [7, 8]

$$\mathcal{H}_{\mathrm{DM}} = \sum_{i>j} \mathbf{D}_{ij} \cdot [\mathbf{S}_i \times \mathbf{S}_j] \ , \tag{4}$$

can be introduced. This might be necessary to grasp essential physics, but makes the extraction of parameters, usually from a limited set of experimental data, more ambiguous, leading to a problem of over-parameterization.
It should be noted that the definition of the Heisenberg Hamiltonian in different publications differs sometimes in the sign and in the presence of prefactor 2, that must be taken into account when comparing different sets of extracted parameters. The notation as above corresponds to $J>0$ for the ferromagnetic (FM) coupling.
In the following, the relation of model spin Hamiltonians to first-principles calculations is briefly discussed. The introduction of microscopic concepts, like orbitals, permits to link the exchange constants with the real chemical structure and bonding. Depending on the character of the states involved in the exchange mechanism, one can distinguish between them and quantify the above mentioned concepts like direct exchange, superexchange (indirect exchange) in insulators, itinerant exchange (RKKY interaction) in metals, double exchange in some oxides or anisotropic (Dzyaloshinsky–Moriya) exchange. More details were given by Anderson [9] and Blundell [10].
The advantage of *ab initio* approaches in the extraction of interaction parameters is that certain mechanisms of interaction can be switched on and off in a fully controllable way. Thus, all anisotropy terms may only have effect if the spin-orbit interaction is explicitly present in the calculation. The non-collinear orientation of individual spins can sometimes be arbitrarily chosen, or at least different settings of "up" and "down" configurations of spins with respect to a global quantization axis are available in a calculation scheme, so that angles between spins become in one way or another directly accessible.

2.2 Magnetic interactions

Given the above examples of spin Hamiltonians, one can assume that the magnetic interaction parameters J_{ij} and anisotropy parameters D are the properties of primary interest. Indeed, they are crucial for the behaviour of SMM in question in prospective practical applications, as mentioned above. High J values (if expressed in kT, and compared to envisaged operation temperature) make sure that the spins within the molecule remain coupled and not disorder. High D values make sure that the resulting magnetic moment of a molecule maintains its spatial orientation and cannot be easily rotated due to thermal fluctuations. The quest for high J and D is an important driving force in a search for new better SMM.
Discussing first the magnetic interactions generalized into J, it is important to understand that they are *not* of purely magnetic order, as for instance magnetic dipole interaction would be. Purely magnetic interactions, dipole or quadrupole, are weak and may play a role, say, for establishing a magnetic order throughout a crystal between individual magnetic molecules, which are often separated by long organic fragments. On the contrary, much stronger intramolecular interactions occur via chemical bonds, and they are electrostatic in their nature. The mutual arrangement of spins happens due to an interplay between Coulomb interaction and Pauli exclusion principle, in what is referred to as *exchange interaction*. The attraction by atomic nuclei and repulsion by other electrons governs the arrangement of electronic states in molecular orbitals, whereby the Pauli principle demands that only two electrons with opposite spin may share the

same orbital. The simple case of two electrons helps to understand why this interaction is called exchange. Given two non-interacting electrons at $\mathbf{r}_1$ and $\mathbf{r}_2$ with their respective wave functions $\varphi_1(\mathbf{r}_1)$ and $\varphi_2(\mathbf{r}_2)$, we can build up a trial two-electron wave function from the products of the latter. As the electrons are indistinguishable, the probability density should remain unaffected if we exchange them; this leaves the only possibilities of either fully symmetrized (S) or fully antisymmetrized (AS) combinations of φ_1 and φ_2:

$$\begin{aligned} \psi_{\rm S}(\mathbf{r}_1,\mathbf{r}_2) &= \frac{1}{\sqrt{2}}\left[\varphi_1(\mathbf{r}_1)\varphi_2(\mathbf{r}_2)+\varphi_1(\mathbf{r}_2)\varphi_2(\mathbf{r}_1)\right] ; \\ \psi_{\rm AS}(\mathbf{r}_1,\mathbf{r}_2) &= \frac{1}{\sqrt{2}}\left[\varphi_1(\mathbf{r}_1)\varphi_2(\mathbf{r}_2)-\varphi_1(\mathbf{r}_2)\varphi_2(\mathbf{r}_1)\right] . \end{aligned}$$

So far we considered only the spatial component of the wave function, but the electrons are also characterized by a spin. In fact the complete wave function for electrons $\psi(\mathbf{r}_1,\sigma_1;\mathbf{r}_2,\sigma_2)$, including spatial and spin components, must be antisymmetric, hence we have two possibilities: an antisymmetric spin singlet state S ($S=0$) together with a spatial symmetric state, or symmetric spin triplet T ($S=1$) with an antisymmetric spatial part:

$$\psi(\mathbf{r}_1,\sigma_1;\mathbf{r}_2,\sigma_2) = \begin{cases} \chi_{\rm S}(\sigma_1,\sigma_2)\,\psi_{\rm S}(\mathbf{r}_1,\mathbf{r}_2) , \\ \chi_{\rm T}(\sigma_1,\sigma_2)\,\psi_{\rm AS}(\mathbf{r}_1,\mathbf{r}_2) . \end{cases} \tag{5}$$

The energy difference between the singlet $E_{\rm S}$ and the triplet $E_{\rm T}$ states allows to define the exchange constant J between the spins,

$$J = \frac{E_{\rm S}-E_{\rm T}}{2} . \tag{6}$$

A positive value of J ($E_{\rm S} > E_{\rm T}$) favours the triplet state with $S=1$; $J<0$ – the singlet one.
Where does the difference between energies of singlet and triplet states come from? Obviously it is determined only by spatial shape of $\psi_{\rm S}$ and $\psi_{\rm AS}$. Some general ideas about the sign of J, with the use of kinetic energy and Coulomb repulsion arguments, have been given by Anderson [9]. Let us assume that there are two electrons on the same atom. The spatially antisymmetric wave function minimizes the Coulomb repulsion, because the two electrons are spatially separated. Hence the spin triplet state is lower in energy, J is positive, and the resulting ferromagnetic-like interaction between the spins is consistent with Hund's first rule. Another enlightening example is represented by two electrons on neighboring atoms, so that they can form bonds. The corresponding molecular orbitals can be spatially symmetric (bonding) or antisymmetric (antibonding) as outlined above. The antibonding orbital has larger kinetic energy (larger curvature, on the average), which implies that it is energetically more expensive. This favours the spin-antisymmetric singlet state with the spatially symmetric bonding molecular orbital, hence the exchange constant is negative resulting in an antiferromagnetic-like interaction.
While this concept is straightforward for two electrons, the extension to many electrons becomes complicated. Still it provides a useful starting point for further qualitative discussion of exchange in many-electron systems.
As a further refinement when discussing exchange interactions through chemical bonds, one has to distinguish between direct exchange (due to an immediate overlap of atomic states of magnetic atoms) or indirect one, occurring via an intermediate atom or group of atoms (diamagnetic groups), which form an *exchange path* of coupled chemical bonds. Whereas the direct exchange is crucial for transition metals (TM) and alloys, the physics of molecular magnets, as also in TM oxides, is governed by indirect exchange.

A concept of *double exchange*, introduced by Zener [11] in order to explain FM ordering in conducting complex oxides, and further elaborated by Anderson and Hasegawa [12], might turn out helpful for some SMM, and a profound discussion on "superexchange", a term coined by Anderson [13] for *insulating* (and usually antiferromagnetic) TM oxides – for some other SMM. The starting point of Anderson's analysis is the introduction of localized magnetic orbitals, related to a certain TM ion but including also some electron states of a diamagnetic ligand. Different magnetic orbitals may therefore share a common ligand and either experience an overlap there, or be orthogonal. The simple argument of Anderson is "that antiparallel electrons can gain energy by spreading into non-orthogonal overlapping orbitals, where parallel electrons cannot". This is generalized in form of the Goodenough-Kanamori(-Anderson) rules [14–16], stating that if two electrons are in orbitals that directly overlap, their exchange (i.e., the 180°-exchange) is strong and of AFM type, whereas for the (interacting) orbitals which are orthogonal, the (90°-)exchange is weak and of the FM type. The real world might however deviate from these rules.

2.3 Relation to first-principles calculations

Each of the above cited models for exchange provide an internal parametrisation of the resulting J in terms of, say, Coulomb integral, overlap of different orbitals and transfer probabilities. However, it is not a good idea to rely on such parameters as estimated from *ab initio* calculations, because of ambiguities in their definition – which wave functions to use, how to account for screening effects, etc.

More promising strategy is a "low-level" parameterization of the interaction energy directly in terms of few basic observables. A good example is the Heisenberg model which casts the interaction of (presumably well defined) spins into a simple analytical form, incorporating all underlying physics in a single isotropic interaction parameter. An advantage of introducing such parameters (of interaction between nominal spins) is that they are better accessible in experiment. For example, the calculated Heisenberg exchange parameter would have the same meaning as that extracted from observed Curie-Weiss behavior of measured magnetic susceptibility. The disadvantage is that the underlying physics, whether the obtained interaction comes about due to superexchange, double exchange or whatever, remains somehow hidden. This disadvantage is actually not so serious, because once the calculation is done, a careful analysis of its results – energies, wave functions etc. – might recover a good deal more useful information than merely interaction parameters. The issues of hybridization, localization, charge transfer are typical ingredients of a quantum chemical analysis, and normally they do give insight into the origin of a particular magnetic ordering. If we understand them, we may hope to find possibilities to "design" or at least to influence the magnetic properties.

By first-principles calculations we mean those which attempt to solve the most general quantum-mechanical equations, i.e. either Schrödinger or Dirac equation, for a system of either fixed, or movable point-charge nuclei, accommodating many electrons. For cases more complex than a hydrogen-like (one-electron) ion, analytical solution is not possible. The necessary approximations can be divided into conceptual and technical ones. The former are about reducing the underlying physical problem to a feasible one; such was the Hartree–Fock (HF) approximation, casting the many-electron wave function $\Psi(\mathbf{r}_1, \ldots, \mathbf{r}_N)$ as a single Slater determinant, and introducing the mean-field concept. Systematic improvements of the HF scheme, which make use of multi-determinantal wave functions, constitute the domain of *quantum chemistry* (QC).

Another example is density functional theory (DFT), a reliable working horse in practical elec-

tronic structure calculations since 1960s – see Dreizler and Gross [17], Eschrig [18] for reviews. Its central idea is the removal of many-electron wave function from the picture whatsoever, putting at its place the one-electron density

$$\rho(\mathbf{r}) = \int \Psi^*(\mathbf{r}, \mathbf{r}_2, \cdots, \mathbf{r}_N)\, \Psi^*(\mathbf{r}, \mathbf{r}_2, \cdots, \mathbf{r}_N)\, d\mathbf{r}_2 \cdots d\mathbf{r}_N$$

as subject to variation in the search for the total energy of the ground state. It turned out useful, as was proposed by Kohn and Sham [19], to express the searched for density $\rho(\mathbf{r})$ via fictitious functions $\psi_i(\mathbf{r})$, which are postulated to be wavefunctions of non-interacting quasiparticles without apparent physical meaning, but possessing the same density as the true physical system:

$$\rho(\mathbf{r}) = \sum_{\alpha=1}^{N} |\psi_\alpha(\mathbf{r})|^2 \,. \tag{7}$$

The variational principle applied to wavefunctions $\psi_i(\mathbf{r})$ leads to a set of Kohn-Sham equations:

$$\left[-\frac{\hbar^2}{2m}\nabla^2 + U(\mathbf{r}) + \int \frac{\rho(\mathbf{r}')\, d\mathbf{r}'}{|\mathbf{r} - \mathbf{r}'|} + \frac{\delta E_{\mathrm{XC}}[\rho]}{\delta \rho(\mathbf{r})} \right] \psi_\alpha(\mathbf{r}) = \epsilon_\alpha\, \psi_\alpha(\mathbf{r}) \,. \tag{8}$$

DFT claims to be an exact theory *in principle*, at least in what regards the treatment of ground-state properties. However in practical terms, in order to specify the exchange-correlation term $\delta E_{\mathrm{XC}}[\rho]/\delta\rho(\mathbf{r})$ in the above Kohn–Sham equations, one has to choose one or another parametrisation. This gives rise to different "flavours" of DFT, like local density approximation (LDA), generalized gradient approximation (GGA), etc. The lecture by R. Zeller on band magnetism offers a more extended covering of DFT.

Approximations of technical kind are about how to accomplish the necessary "number crunching" in a more efficient way, without big loss of accuracy. This covers the choice of adequate computation scheme with its choice of basis, representation of potential and charge density, performing necessary integrations, etc. Among a large variety of calculation schemes being developed since decades, not all are well suited for simulations on molecular magnets. Several examples will be discussed below in Section 3.

Turning now to the problem of evaluating the parameters of spin Hamiltonians from first principles, we note that in executing the calculation one has the freedom to impose certain constraints (fix the magnitude or orientation of magnetization, modify the potential felt by certain electronic states, switch on or off the relativistic effects) and inspect the effect of these constraints on the total energy. Moreover, one-electron eigenvalues and corresponding (Kohn-Sham, or Hartree-Fock) eigenfunctions are also available from a self-consistent calculation. There are certain subtleties related to the extraction of exchange parameters from QC and DFT calculations which one should be aware of.

In QC one deals with a multi-configurational scheme which allows to mix different spin configurations and to classify energy eigenvalues according to different total spin values. For two interacting spins $\mathbf{S}_1$, $\mathbf{S}_2$ summing up to $\mathbf{S}' = \mathbf{S}_1 + \mathbf{S}_2$ one gets

$$2\mathbf{S}_1\mathbf{S}_2 = \mathbf{S}'^2 - \mathbf{S}_1^2 - \mathbf{S}_2^2 \,,$$

with eigenvalues $[S'(S'+1) - S_1(S_1+1) - S_2(S_2+1)]$. For a textbook example $S_1 = \frac{1}{2}$, $S_2 = \frac{1}{2}$ this yields a singlet $(S' = 0)$ and a triplet $(S' = 1)$ states. The corresponding eigenvalues of the Heisenberg Hamiltonian must be then $3/2J$ and $-1/2J$, correspondingly.

Indeed, the basis functions in an *ab initio* calculation are normally pure spin states. In the basis of spin functions $|m_{S_1} m_{S_2}\rangle$, for the case $S_1 = \frac{1}{2}$, $S_2 = \frac{1}{2}$ the Heisenberg Hamiltonian takes the form:

$$\begin{array}{c|cccc} m_{S_1} m_{S_2} & \left|\, \frac{1}{2}\ \frac{1}{2}\right\rangle & \left|-\frac{1}{2}\ \frac{1}{2}\right\rangle & \left|\, \frac{1}{2}-\frac{1}{2}\right\rangle & \left|-\frac{1}{2}-\frac{1}{2}\right\rangle \\ \hline \left|\, \frac{1}{2}\ \frac{1}{2}\right\rangle & -J/2 & & & \\ \left|-\frac{1}{2}\ \frac{1}{2}\right\rangle & & J/2 & -J & \\ \left|\, \frac{1}{2}-\frac{1}{2}\right\rangle & & -J & J/2 & \\ \left|-\frac{1}{2}-\frac{1}{2}\right\rangle & & & & -J/2 \end{array} \tag{9}$$

The diagonalisation of (9) is achieved by a basis transformation which mixes different m_S values:

$$\begin{array}{l} \frac{1}{\sqrt{2}}\left(\left|\, \frac{1}{2}\ -\frac{1}{2}\right\rangle - \left|-\frac{1}{2}\ \frac{1}{2}\right\rangle\right) \qquad \text{(singlet)} \quad S=0 \quad E=\frac{3}{2}J\ ; \\ \left.\begin{array}{l} \left|\, \frac{1}{2}\ \frac{1}{2}\right\rangle \\ \frac{1}{\sqrt{2}}\left(\left|\, \frac{1}{2}\ -\frac{1}{2}\right\rangle + \left|-\frac{1}{2}\ \frac{1}{2}\right\rangle\right) \\ \left|-\frac{1}{2}\ -\frac{1}{2}\right\rangle \end{array}\right\} \quad \text{(triplet)} \quad S=1 \quad E=-\frac{1}{2}J\ . \end{array} \tag{10}$$

In a QC (multi-determinantal) calculation the eigenvalues of singlet and triplet states, E_{S} and E_{T}, are immediately accessible. This allows the (formal yet unambiguous) mapping of a first-principles result onto the Heisenberg model:

$$E_{\mathrm{S}} - E_{\mathrm{T}} = 2J\,, \tag{11}$$

identically with the above discussed model case of two electrons (6). The case $S_{1,2} = \frac{1}{2}$ corresponds to, e.g., two interacting Cu^{2+} ions. Other ions from the $3d$ row yield richer systems of eigenvalues – for instance, $S_{1,2} = 1$ (two Ni^{2+} ions) produces a quintet level E_{Q} beyond singlet and triplet, with the energy separation

$$E_{\mathrm{S}} - E_{\mathrm{Q}} = 6J\,. \tag{12}$$

Whether both equations (11) and Eq. (12) can be satisfied by the same J is a measure of validity of the Heisenberg model.

In DFT, the search for the "true" wave function is avoided and substituted by the variational search for the charge density and total energy. As the eigenvalues of multi-determinantal states are not available, one must either rely on the Kohn-Sham eigenvectors or on total energies in specially prepared symmetry-breaking metastable states, subject to different constraints with respect to the spin states of a system. In practice, one can try ferromagnetic (FM) or antiferromagnetic (AFM) configurations of two spins, or impose the fixed spin moment (FSM) scheme, first introduced by Schwarz and Mohn [20]. The total energy in different spin configurations does *not* relate to the eigenvectors but to diagonal elements of, e.g., the Hamiltonian $\mathcal{H}$ of (9):

$$\begin{aligned} E_{\mathrm{FM}} &= \left\langle \frac{1}{2}\ \frac{1}{2}\right|\ \mathcal{H}\ \left|\frac{1}{2}\ \frac{1}{2}\right\rangle = -\frac{1}{2}J\,, \\ E_{\mathrm{AFM}} &= \left\langle -\frac{1}{2}\ \frac{1}{2}\right|\ \mathcal{H}\ \left|-\frac{1}{2}\ \frac{1}{2}\right\rangle = \frac{1}{2}J\,, \end{aligned} \tag{13}$$

hence

$$E_{\mathrm{AFM}} - E_{\mathrm{FM}} = J \tag{14}$$

for the above case of $S_{1,2} = \frac{1}{2}$. This is a valid representation for J provided the Heisenberg model itself remains valid throughout the path from FM to AFM state. The latter formula can be approximated using the concept of magnetic transition state [21]. Generally, according to Slater, the shift in the DFT total energy ΔE due to a whatever change Δn_i in the occupation of certain orbitals is

$$\Delta E = \sum_i \Delta n_i \varepsilon_i^* + \mathcal{O}(\Delta n^3)\,, \tag{15}$$

where ε_i^* are Kohn-Sham eigenvalues obtained self-consistently with occupation numbers midway between initial and final states. For the flip from FM to AFM configuration,

$$E_{\mathrm{FM}} - E_{\mathrm{AFM}} \simeq \sum_i \left(n_{i\uparrow}^A - n_{i\downarrow}^A\right)\left(\varepsilon_{i\downarrow}^* - \varepsilon_{i\uparrow}^*\,,\right) \tag{16}$$

where $(n_{i\uparrow}^A - n_{i\downarrow}^A)$ is the magnetic moment (which gets inverted) in the orbital i. The latter bracket is the spin splitting (in energy) of the same orbital, calculated in the configuration with zero spin on atom A (transition state), i.e. induced fully via the interaction with the second spin. While being approximative, the magnetic transition state scheme might have a certain advantage of numerical stability over explicit comparison of large total energy values. Moreover, the result is available from a single calculation and offers a microscopical insight of how different orbitals are affected by magnetic interaction – information which remains hidden in the total energy numbers. Being of use a number of times in the past (primarily for magnetic oxides), the method has recently been applied to the analysis of exchange parameters in Mn_{12}-ac [22].

The validity of either "finite difference" scheme (14), or "differential" procedure (16) presumes that the mapping onto the Heisenberg model makes sense in the first place. However, with just two interacting spins we have no immediate criterion whether this is true. The applicability of the Heisenberg model would mean that the functional part of the interaction comes from the scalar product of two spin operators, with the parameter J_{ij} being independent on $\mathbf{S}_i$ and $\mathbf{S}_j$. The mapping on the Heisenberg model may be less ambiguous if done as a limiting case of small deviations from a certain stationary state. The meaning of such deviations in the DFT might be some admixture to pure spin states (in the sense of local spin density functional), i.e., non-diagonal (in the spin space) form of density matrices. It allows a transparent quasi-classical interpretation in terms of non-collinear magnetic density varying from point to point in space – see Sandratskii [23] for a review. If a pair of local magnetic moments can be reasonably identified in the calculation, and their small variations from the global magnetization axis are allowed, the counterparts in the Heisenberg model will be deviations of local exchange fields at two corresponding sites. Matching the leading terms in the angular dependence of interaction energy in the DFT and in the Heisenberg model yields the desired mapping:

$$J_{ij} = \sum_{\{m\}} \Delta^i_{mm'}\, \chi^{ij}_{mm'm''m'''}\, \Delta^j_{m''m'''} \tag{17}$$

where Δ^i is the spin-splitting of the on-site potential, possibly non-diagonal in the expansion over spherical harmonics around a given center, and χ^{ij} is non-local susceptibility, specified in Appendix 1 in terms of eigenvalues and eigenfunctions. The line of arguing resulting in Eq. (17) goes back to at least Oguchi et al. [24] who extracted interaction parameters in simple $3d$ oxides from DFT calculations. Liechtenstein *et al.* [25–27] worked out closed expression for J_{ij} in a form consistent with spin-fluctuation theories, in terms of the elements of the Green's function (see Appendix 1).

2.4 Spin-orbit coupling and magnetic anisotropy energy

It was earlier mentioned that high anisotropy values are essential to ensure that the resulting magnetic moment of a SMM maintains its spatial orientation and cannot be easily rotated due to thermal fluctuations. Together with high magnetic excitation parameters, it is therefore an important "figure of merit" for various applications of molecular magnets. In general, the magnetocrystalline anisotropy reflects the energy difference for different possible orientations of spins with respect to crystallographic axes. Such discrimination may only occur via the spin-orbit coupling and hence is a manifestation of relativistic effects in the electronic structure. Well known for bulk magnetic materials, magnetic anisotropy determines the preferential type of magnetization of a sample and fixes, in the most general case, its easy, medium and hard magnetic axes. A special case is uniaxial anisotropy when the energy depends only on the angle to one certain axis, irrespectively to the direction of other two. The preferential orientation of magnetization along this selected axis is referred to as "easy axis" type of anisotropy; the opposite case, when the magnetization accommodates itself normally to the selected direction, is called "easy plane". In any case the magnitude of the energy variation while scanning different directions of magnetization is quite small, of the order of 10^{-3}–10^{-6} eV per atom.
In cubic systems the second order contributions to the anisotropy energy vanish by symmetry, so that like in bulk Fe, Co or Ni there will be only 4th order contributions which are very small. Most molecular nanomagnets are low-symmetric, therefore the second order anisotropy is present in them, achieving in some cases the values of several K.
Recently, Pederson and Khanna [28, 29] have developed a method for accounting for second-order anisotropy energies (see Appendix 2). In the absence of a magnetic field, the second-order perturbative change to the total energy of a system with arbitrary symmetry becomes

$$\Delta_2 = \frac{1}{4}\sum_i M_{ii}^{12} + M_{ii}^{21} + \sum_{ij}(M_{ij}^{11} + M_{ij}^{22} - M_{ij}^{12} - M_{ij}^{21})\frac{\langle S_i\rangle\langle S_j\rangle}{(\Delta N)^2}. \qquad (18)$$

Here i, j run over sites, 1 or 2 label spin directions, $M_{ij}^{\sigma\sigma'}$ accumulate the matrix elements of the potential between occupied and unoccupied states, ΔN is an excess number of majority-spin electrons – see Appendix 2 for details. Section 4 below overviews the applications of this formula for some systems of actual interest.

3 Calculation difficulties and suitable calculation schemes

Beyond the conceptual approximations adopted for solving the many-electron problem, as discussed in Sec. 2.3, e.g., HF approximation, QC multi-determinantal approach, or Kohn-Sham equations, one has to choose how to solve the corresponding equations numerically. This involves additional approximations, which are of purely technical character, but demand a fair amount of physical insight and programming sophistication in order to combine accuracy with feasibility of the calculations. In virtually all cases one has to decide first on an appropriate set of *basis functions* $\chi_p(\mathbf{r})$ used to expand the sought for one-electron orbitals $\psi_\alpha(\mathbf{r})$, which enter the Kohn-Sham equations (8):

$$\psi_\alpha(\mathbf{r}) = \sum_{p=1}^{Q} C_{\alpha p}\chi_p(\mathbf{r})\,. \qquad (19)$$

This expansion is always finite, but the dimension of the basis Q must be reasonably larger than the number of occupied electronic states N, for providing sufficient flexibility in the variational

search for the solution of either Kohn-Sham, or HF equations. The two most common choices of $\chi_p(\mathbf{r})$ are plane waves and atom-centered localized functions. The former are defined as

$$\chi_{\mathbf{G}}(\mathbf{r}) = \frac{1}{\sqrt{\Omega}}\, e^{i\mathbf{G}\mathbf{r}}\,, \tag{20}$$

i.e. labeled by vectors $\mathbf{G}$ of the reciprocal lattice, which corresponds to a periodic unit cell of volume Ω. Such a periodic cell (simulation box) must always be introduced for calculations with planewave basis sets, even if the simulated system is in reality not periodic (e.g., a single molecule). The number of planewave basis functions needed for sufficient accuracy grows rapidly with the size of the simulation box, independently on the actual number of atoms contained in the box. The planewave basis (see, e.g., Ref. [30] for more details) has the advantage of becoming ultimately complete under the variation of a single cutoff parameter, $G_{\max}$, since it includes all planewaves with $|\mathbf{G}| \leq G_{\max}$. The planewave cutoff energy can be kept reasonably low by using, instead of true (deep near the nuclei) Coulomb potentials, screened pseudopotentials and correspondingly smoothed pseudofunctions for electrons in valence shells, thus excluding the core states from the calculation.

The atom-centered functions, on the contrary, are better suited for describing strong spatial fluctuations of the one-electron functions within atoms and hence allow much smaller (and even almost minimal, $Q \gtrsim N$) basis sizes. However they face problems, or at least ambiguities, in a consistent generation of efficient basis sets, and in performing spatial integrations. The atom-centered functions can be further divided into numerical and analytical ones, energy dependent or not, fixed or adjustable in the course of iterating the Kohn-Sham equations to self-consistency. A common workable choice among fixed analytical basis functions are Gaussian-type orbitals – see, e.g., [31] for a review.

Recently, there was a notable increase in the number of calculations which solve the underlying equations on a real-space grid [32, 33], with finite differences or finite elements technique [34, 35]. Yet this is equivalent to the use of piecewise linear or polynomial functions, localized at grid points, as a basis. Attempts to combine the advantages of planewave and localized-basis techniques resulted in a number of high-precision calculation schemes, like the full-potential linearized augmented plane wave (FLAPW) [30, 36] or the projected augmented-wave [37, 38] methods. In essentially all calculation schemes, the introduction of the basis expansion (19) reduces the system of coupled integro-differential equations Kohn-Sham equations (8) to a generalized eigenvalue problem:

$$\sum_p C_{\alpha p} \left[\int \chi_q^*(x) \mathcal{H} \chi_p(x) dx - \varepsilon_\alpha \int \chi_q^*(x)\, \chi_p(x)\, dx \right] = 0\,, \tag{21}$$

where $\mathcal{H}$ is the operator acting at the function $\varphi_\alpha(\mathbf{r})$ or $\psi_\alpha(\mathbf{r})$ on the left side of Eq. (8). In most cases (basis functions either energy-independent, or only linearly dependent on energy) the remaining technical problem reduces to the evaluation of matrix elements of the Hamiltonian $\mathcal{H}$ and of the overlap, and the diagonalisation. After solving the matrix equations one can calculate the electron density (7) and the total energy, which are the basic characteristics of the ground state. A number of other properties (spin density, forces on atoms, vibrational frequencies) may be calculated as well.

The physical questions which are of interest in the study of molecular magnets are not intrinsically different from those encountered in the study of magnetism and electronic structure of, say, bulk solids, surfaces, of clusters from first principles in the DFT. One is interested in a

description of the ground-state electronic structure and, as far as possible, of the lowest excitations, in terms of Kohn-Sham eigenvalues and the corresponding charge and spin density. The simulation of molecular magnets presents, however, certain technical difficulties which are not necessarily typical for all DFT applications, and impose limitations both on the choice of the computational code for an efficient use and on the number of systems addressed so far in a first-principle simulations. These difficulties are:

• large number of atoms, up to several hundreds of atoms per repeated structural unit;

• low or no symmetry, which makes it difficult to split the generalized eigenvalue problem (Eq. 21) into symmetry-resolved smaller blocks;

• large size of a simulation box, that means large number of plane waves is needed, if they are used as basis functions;

• an important role of "heavy" atoms with deep core states and sometimes with important semicore – this may create difficulties for the use of pseudopotential-based methods;

• the lack of energy dispersion (due to very week coupling between molecular units) and quite commonly a dense spectrum of nearly degenerate discrete states in the vicinity of HOMO-LUMO gap, which makes the self-consistency slowly convergent or even unstable.

Retrospectively, it seems understandable that a large number of calculations done so far employed one or another scheme using flexible tight-binding bases. Pseudopotential planewave calculations are not much represented so far. An accurate all-electron FLAPW method, a recognized tool of choice when dealing with different "conventional" solids, faces its specific problems in treating atoms of very different size in the same calculation, as it is needed for molecular magnets. So far such schemes were used only for benchmark calculations on simplified systems.

Coming down to "hands-on" calculation tools, we'll see that several calculation methods have been so far applied with considerable impact in the studies of molecular magnets. Boukhvalov *et al.* used the **The Tight-Binding Linear Muffin-Tin Orbital method** (TB-LMTO, see [39–41]) for their calculations of electronic structure and magnetic interaction parameters in Mn_{12}-ac [42] and V_{15} [43]. The interatomic exchange parameters J were estimated along Eqs. (17) and (34). The TB-LMTO method employs flexible basis of numerical functions, which are adjusted in the course of approaching the convergence; the method is fast, robust and normally provides reasonable description of the electronic structure even in complex materials. Weak features of the method are the spherical-symmetric averaging of the potential inside *atomic spheres* circumscribing each atom, an approximation not good enough to allow a reliable calculation of forces and relaxation of structure. Moreover the treatment of open systems demands to pack large interstitial space with *empty spheres*, a cumbersome, ambiguous and seldom satisfactory procedure. These deficiencies are known to degrade delicate results of calculation, such as accurate placement of some bands, or fine details of their dispersion in solids.

Boukhvalov et al. emphasize the importance of intraatomic correlation for correct description of magnetic interactions and excitation spectra of Mn_{12}-ac and V_{15}. Technically the desirable correction is provided by the LDA+U [44] *ansatz*, implemented in the Yekaterinburg version of the TB-LMTO code and nowadays part of many other calculation codes. In the LDA+U scheme, the interaction energy within a certain *ad hoc* chosen group of states, which are expected to be particularly localized and hence "correlated" (typically, transition metal d states) is accounted for like in the Anderson model, with appropriately chosen average Coulomb interaction parameter U and occupations of affected one-electron states n_i. For these selected states only, the model treatment of interaction among such "correlated" electrons substitutes the conventional mean field-like DFT treatment – say, within the local densitzy approximation, LDA.

Such a correction in a simplified case, without accounting for a degeneracy within the affected subsystem of N electrons yields

$$E^{\mathrm{LDA}+U} = E^{\mathrm{LDA}} - \frac{1}{2}UN(N-1) + \frac{1}{2}U\sum_{i\neq j} n_i n_j \,. \tag{22}$$

There are certain arguments for the choice of the parameter U in the above mentioned papers, one recommends $U \approx 4$ eV for V_{15} and $U \approx 8$ eV for Mn_{12}-ac. As the magnitude of U is in fact a free adjustable parameter of a calculation, it often makes sense to vary it, checking its effect on the results. For Mn_{12}-ac one finds that on varying U from 4 to 6 to 8 eV, the exchange interaction parameters between the four inner Mn atoms of the Mn_{12}-ac core vary from 37 to 33 to 30 K (other Mn–Mn interaction constants, of the same order of magnitude, change in a similar manner). Moreover, the local magnetic moments on all Mn atoms become slightly enhanced, and the band gap increases from 1.35 to 1.78 to 2.01 eV. In a minute we'll compare these results with what provide other calculation methods for the same system.

Another method, or rather a whole large family thereof, use basis sets constructed from atom-centered **Gaussian-type orbitals**. These orbitals are not so flexible and efficient as numerical basis functions, but they have wonderful mathematical properties enabling easy analytical manipulations, including analytical evaluation of many related spatial integrals. The methods in question can be referred to as "full-potential" ones, in the sense that no muffin-tin or atomic spheres geometry is imposed, and the spatial form of the potential is fairly general. In particular the version implemented in the Naval Research Laboratory Molecular Orbital Library (NRLMOL) code [45–47] has been frequently used in calculations on molecular magnets. The NRLMOL program package developed by Pederson, Jackson and Porezag is an all-electron Gaussian-type orbital implementation of DFT [45, 46, 48–51]. By including the spin-orbit coupling it is possible to calculate the magnetic anisotropy energy, as outlined above in Sec. 2.4. The agreement between experiment and the result from the first-principles calculation is in many cases surprisingly good (see Sec. 4.4 below).

The **Discrete variational method** (DVM) [52, 53], one of the earliest DFT schemes to find applications in chemistry, seems to be potentially very well suited for the studies of molecular magnets. The method is an all-electron one, it uses basis of numerical atomic orbitals, and an efficient scheme of 3-dimensional spatial integration, using a pseudorandom numerical grid. DVM was used quite early for first-principles calculations of the electronic structure of a large molecular magnet such as the 10-member "ferric wheel" [54].

It so happened that all three methods discussed above have been applied to the calculation of electronic structure and the evaluation of magnetic interaction parameters of Mn_{12}-ac, a molecule shown in Fig. 1. An overview of results, resolved over three structurally inequivalent groups of Mn atoms – Mn(1) in the inner cube, Mn(2) and Mn(3) in the peripheral region, and the couplings between members of these groups – is given in Table 1. Differences should be noted in the meaning of data obtained by different calculation methods. Local magnetic moments are attributed to the spin density integrated over an atom-centered sphere of certain radius (TB-LMTO, NRLMOL) or to the Mulliken popultion analysis (DVM). Exchange parameters J have been extracted in the TB-LMTO calculation [42] by using the formula (17), whereas in the NRLMOL calculation [55] – by fitting the total energies from several trial spin configurations onto the Heisenberg model. Finally, Zeng et al. in their DVM calculation [22], one of the first *ab initio* studies of the Mn_{12}-ac, estimated Heisenberg exchange parameters in the magnetic transition state scheme [21], an extension of Slater's original transition state *ansatz*, through a procedure outlined above in Sec. 2.3. Flipping the spin at one atom and detecting the shift of

Table 1: *Electronic structure parameters (magnetic moments and Heisenberg exchange parameters) of Mn_{12}-ac from ab initio calculations by three different methods.*

Method	Magnetic moments (μ_B)			Exchange parameters (K)		
	Mn(1)	Mn(2)	Mn(3)	J_{12}	J_{13}	J_{23}
DVM[a]	3.056	−3.889	−4.039	−136	−72	−102
NRLMOL[b]	2.57	−3.63	−3.58	−57	−41	−8
LMTO[c], U=4 eV	2.72	−3.44	−3.65	−53	−47	−19
LMTO[c], U=8 eV	2.92	−3.52	−3.84	−47	−26	−7

[a]Ref. [22]; LDA.
[b]Ref. [29]; GGA; moments within a sphere of 2.5 Bohr. J values by Park et al. [55].
[c]Ref. [42]; LDA+U; moments within spheres of 2.7/2.8 Bohr (inner/outer Mn atoms).

the $3d$-energy level on another one due to induced magnetic polarization helped to arrive at a system of equations in which different interatomic exchange parameters were coupled. For the sake of simplicity and the clearness of analysis, only collective (non-symmetry-breaking) spin flips on all atoms belonging to each set of Mn atoms were allowed in the analysis of Zeng et al.. This means that four spins within each group always remained rigidly ferromagnetically coupled. This resulted in a system of three equations, whence the values of J_{12}, J_{23} and J_{13} could have been determined. The DFT results were explicitly fitted to the Heisenberg Hamiltonian of the form of Eq. (1). However, the parameters J_{11} etc., representing the coupling within each group, did not appear in the fit, because the spin excitations necessary to probe them, which would break the symmetry of the molecule, were not allowed. Their inclusion in an otherwise executed calculation could result in a renormalization of exchange parameters.
The values of J_{12}, J_{23} and J_{13} are given in Table 1; they are all negative, i.e. indicate an AFM coupling (as could be expected due to a more-than-90° superexchange pathway through bridging oxygens), and hence frustration in accommodating the three spin subsets.
My instrument of choice, at least in what regards the calculations of molecular magnets, is the **Siesta** method and computational code [56–59]. This code again uses compact atom-centered basis functions, but – differently from NRLMOL – numerical ones with strict spatial confinement (see Refs. [60] and [61] for details). Due to a number of smart technical solutions, SIESTA is a great method for treating large low-coordination low-symmetry structures, as molecular magnets exactly are. Differently from the two previously discussed methods, SIESTA is not an all-electron one but employs norm-conserving pseudopotentials. Therefore, as is also true for many other pseudopotential methods, certain care is required in choosing and testing pseudopotentials prior to calculation.
The application of SIESTA to molecular magnets is relatively new. In the following several recent results, obtained with this method, are outlined.

4 Recent calculation results

In the following, some recent results on relatively "new" molecular magnets, i.e. systems which have only become available during the last few years, are outlined. Most of the calculations have

been done with the SIESTA code. The motivation for the study of these systems is manifold. "Ferric wheels" gained interest, not in the last place, because of their beautiful shape and a rich physics they offer in manifesting their quantum properties (see the lecture by J. Schnack). Ni_4 is a seemingly simple magnetic molecule for which a fit of experimental data of magnetization vs. magnetic field to the Heisenberg model fails quite dramatically, and possible reasons for deviation have been studied, with the help of first-principles calculations. Finally, a two-nuclei model system is considered with the aim to study the effect of intraatomic correlation (within the LDA+U approach) on the electronic structure and interatomic magnetic interaction parameters, using a numerically more accurate method (namely, FLAPW) than the TB-LMTO of earlier Mn_{12}-ac calculations by [42]).

4.1 "Ferric wheels"

Hexanuclear "ferric wheels" $M Fe_6[N(CH_2CH_2O)_3]_6Cl$ (M = Li, Na, see Fig. 2), the systems to be discussed below, were synthesized at the Institut für Organische Chemie in Erlangen [62] and labeled as substances **4** and **3** in the latter publication. There exist a large family of ferric wheels with a different even number ($N = 6, 8, 10, 12, 18$) of iron atoms. Besides the ferric ones, there have been reports on wheels with other transition metal ions such as an eight membered Cr(III) wheel [63], Cu(II) [64, 65], Co(II) [66], Mn(II) [67] and a 24 membered Ni(II) wheel [68]. The latter structure contains the largest number of transition metal ions in a wheel-like structure so far. The synthesis of odd-numbered magnetic wheels appears to be a nontrivial task.
Fe atoms in these compounds are connected by oxo-bridges, that are reminiscent of the 90° coupling of magnetic atoms in transition-metal oxides. The nearest coordination of the Fe atom

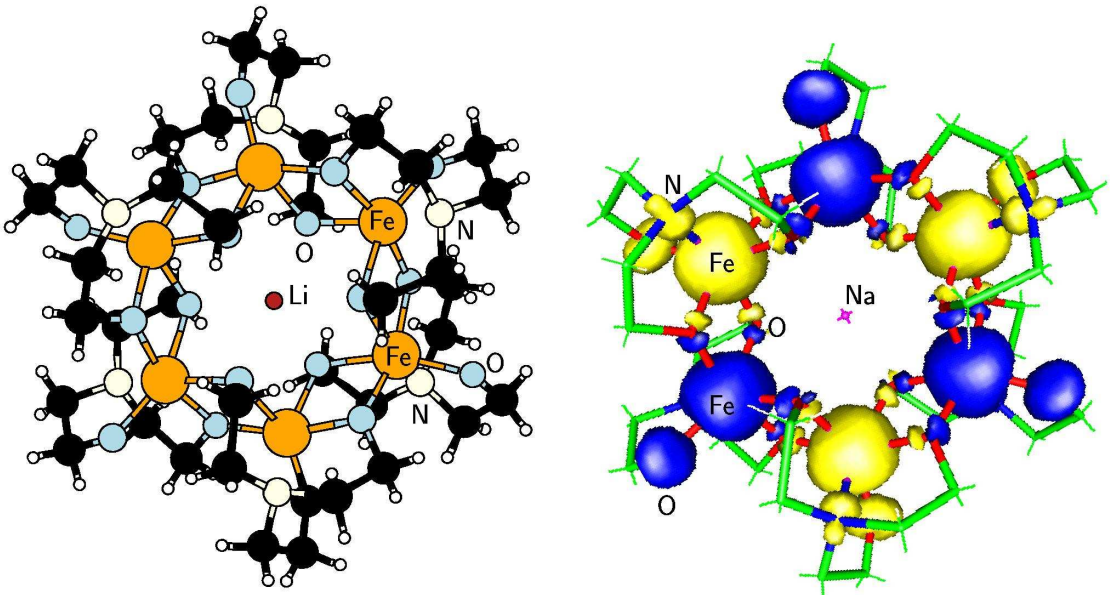

Fig. 2: *Structure and spin density distribution in "ferric wheel" molecules. Left panel: top view of the Li-centered molecule. The Li ion is in the middle of the ring; the distant Cl ion is not shown; the rest of (electrically neutral) solvent is neglected. Right panel: iso-surfaces correspond to $\pm 0.01 e/Å^3$, according to NRLMOL calculation [69]. While most of the magnetic moment is localized at the Fe atoms, there is still some spin polarization on O and N.*

is octahedral; two pairs of O ions form bridges to the neighboring Fe atoms on both sides; the fifth oxygen (referred to below as "apical") and the nitrogen ion are connected by the C_2H_4 group. The octahedra are slightly distorted, to accommodate the stiffness of oxo-bridges with the curvature of the molecular backbone. While the Fe–O–Fe angles differ slightly in the Li-centered and Na-centered wheels (101.1° and 103.3°, respectively), the structure of the two molecules is almost identical.

According to magnetization and torque measurements by Waldmann et al. [70], these systems are characterized by S=5/2 on the Fe site, thus implying a highly ionized Fe(III) state. Moreover, a fit to the spin Hamiltonian of the Heisenberg model (1) yields the J values of -18 to -20 K for the Li-wheel (depending on sample and method) and -22.5 to -25 K for the Na-wheel, thus implying an AFM ground state [70]. X-ray photoelectron and X-ray emission spectroscopy studies [71] allowed for probing of the electronic structure in the valence band and on the Fe site, albeit without resolution in spin. Whereas the magnetic measurements data are by now well established, the spatially resolved distribution of magnetization was not yet accessed prior to calculations by J. Kortus and myself [69]. Specifically, we compared the results of electronic structure calculations by two different methods within the DFT, SIESTA and NRLMOL. In both cases, the generalized gradient approximation after Perdew, Burke, and Ernzerhof [72] was used. The most important difference between two methods, in what regards the present study, is that SIESTA uses norm-conserving pseudopotentials whereas NRLMOL is an all-electron method. The results are however very similar, even as the calculations were in fact performed for two different systems (Li-center wheel by SIESTA vs. Na-centered wheel by NRLMOL, with tiny structural differences). The NRLMOL treatment was restricted to the ground-state AFM configuration (alternating orientations of Fe magnetic moments over the ring); the SIESTA calculation addressed in addition different magnetic configurations, that allowed for the extraction of DFT-based exchange parameters.

Fig. 3 displays the partial densities of states (DOS) on Fe and its several neighbors in the AFM configuration, as calculated by both methods. The discrete levels of the energy spectra are weighted (with the charge density integrated over atom-centered spheres in NRLMOL, or according to Mulliken population analysis in SIESTA), and slightly broadened for better visibility. The local moments corresponding to integrating such partial DOS over occupied states are given in Table 2. Both calculations give a consistent description of state densities at Fe and O sites, even though this property is rather loosely defined, and its calculation differently implemented in SIESTA and NRLMOL.

Notably, both methods find the local magnetic moments on Fe sites very close to 4 μ_B and *not* to 5 μ_B as it is generally assumed, based on the above mentioned magnetization data. The maximal magnetization S=5/2 of the Fe atom corresponds to a Fe(III)-ion with in $3d^5_\uparrow d^0_\downarrow$ configuration. Our first-principles calculations suggest a somewhat different picture: the minority-spin DOS has a non-zero occupation due to the hybridization (chemical bonding) of Fe$3d$ with O$2p$ states. However, the magnetic polarization in the organic ligand which provides the octahedral coordination for the iron atoms, due to Fe is substantial, the most pronounced effect being on the apical oxygen atom (which is not participating in the bonding to the next Fe neighbor). Taken together with the (smaller) polarization of the bridging oxygen atoms and magnetization at the nitrogen site, the distributed magnetic moment *per* Fe atom yields 5 μ_B, recovering the agreement with the magnetization results.

A clear visualization of the above discussed delocalized (or, rather, distributed) magnetic moment associated with the Fe atom comes from the map of spin density, obtained from the NRLMOL calculation (Fig. 2, right panel). One should take into account that the volume enclosed

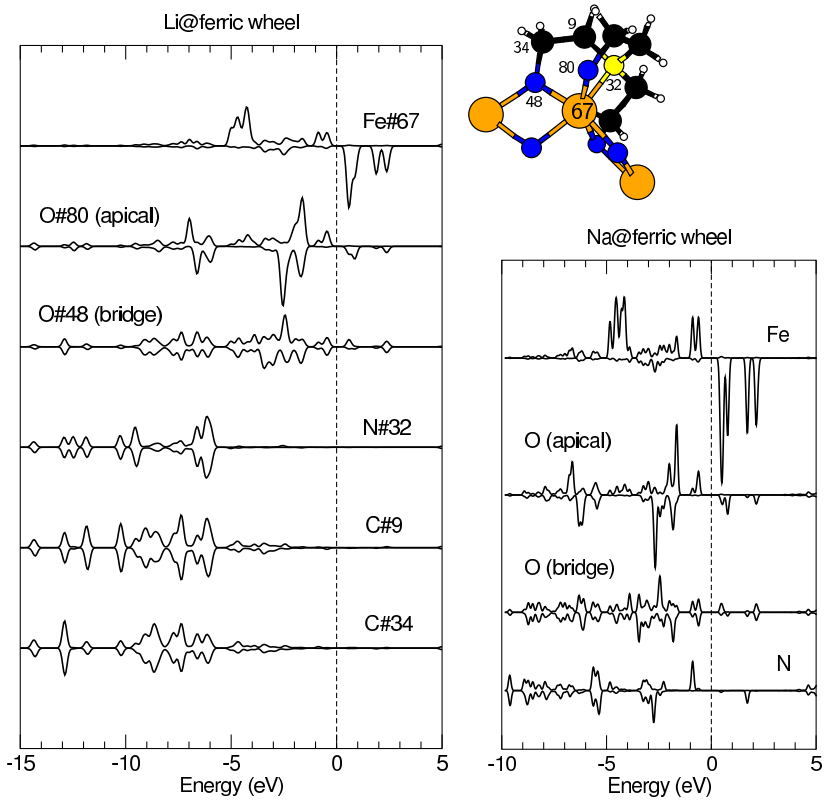

Fig. 3: *Atom- and spin-resolved partial densities of states as calculated for Li-centered molecule by* SIESTA *(left panel) and for Na-centered molecule by NRLMOL (right panel). The DOS at the Fe site is scaled down by a factor of 2 relative to other constituents. The numbering of atoms which are neighbors to the Fe atom is shown in the inset.*

by the iso-surfaces is not directly correlated to the total moment at the site. One sees moreover an absence of magnetization on carbon and hydrogen sites. The fact that the magnetization is noticeable and changes its sign when passing through bridge oxygen atoms emphasizes the failure of methods depending the spherical averaging of atom-centered potentials.

An important consequence is that the charge state of iron is not Fe(III) but more close to Fe(II). Moreover, the distributed magnetic moment behaves like a rigid one, in a sense that it can be inverted, following a spin flip on a Fe site. This is illustrated by the analysis of other mag-

Table 2: *Local magnetic moments M at Fe and its neighbors. NRLMOL results correspond to spin density integrated over sphere of radius R centered at corresponding atom;* SIESTA *values are due to Mulliken population analysis.*

Atom	R(a.u.)	$M(\mu_B)$, NRLMOL	$M(\mu_B)$, SIESTA
Fe	2.19	3.85	3.91
O (apical)	1.25	0.20	0.30
O (bridge)	1.25	$\pm$0.01	$\pm$0.02
N	1.32	0.07	0.09

netic configurations, done with SIESTA [71]. The local DOS does not change considerably when switching from AFM to FM configuration – only the HOMO/LUMO gap becomes less pronounced, and a slight ferro-magnetic shift between the two spin bands appears.

For the sake of improving both the stability of convergence with SIESTA and for pinning down a particular spin configuration (FM, or with one or more Fe magnetic moments inverted), the *fixed spin moment* (FSM, [20]) scheme was applied in the calculation. Imposing an (integer) spin moment per molecule fixes the number of electrons in two spin channels and removes a possibility of spin flips, which are a major source of numerical instability, as there are many nearly degenerate states in the vicinity of the Fermi level in the molecule (and no symmetry constraints on these states in SIESTA). The FSM procedure would normally split the common chemical potential in two separate ones, for majority- and minority-spin channels, that corresponds to an effective external magnetic field and hence to additional (Zeeman) term in the total energy, in analogy with Eq. (3). Since molecular magnets possess a HOMO-LUMO gap, the latter correction must only be considered if such gaps in two spin channels do not overlap.

Fig. 4 shows the total energy values and energy gaps for FSM values of 30 $\mu_{\rm B}$ (FM case), 20 and 10 $\mu_{\rm B}$ (one and two local moments inverted, correspondingly); 0 (alternate-spin AFM case). A linear change of the total energy while inverting one and then two local moments from the FM configuration is what would be expected from the Heisenberg model with "rigid" magnetic moments (in the sense that their S values do not depend on the total spin of the system), assuming moreover that only nearest-neighbors interactions between spins are important. An additional justification of the validity of the Heisenberg model comes from an observation that the magnitudes of local magnetic moments on the Fe atoms always remain close (within several per cent) to 4 $\mu_{\rm B}$, and the partial DOS on Fe sites remains largely unaffected by the actual magnetic ordering. Similarly unaffected is a pattern of local magnetic moments at O and N neighbors of a particular Fe atom, always getting inverted as the latter experiences a spin flip. Keeping this in mind, and assuming Heisenberg-model spin Hamiltonian as in Section 2 with the S value of 5/2 (i.e., for the total spin which gets inverted), we arrive at the estimate for $-J$ of around

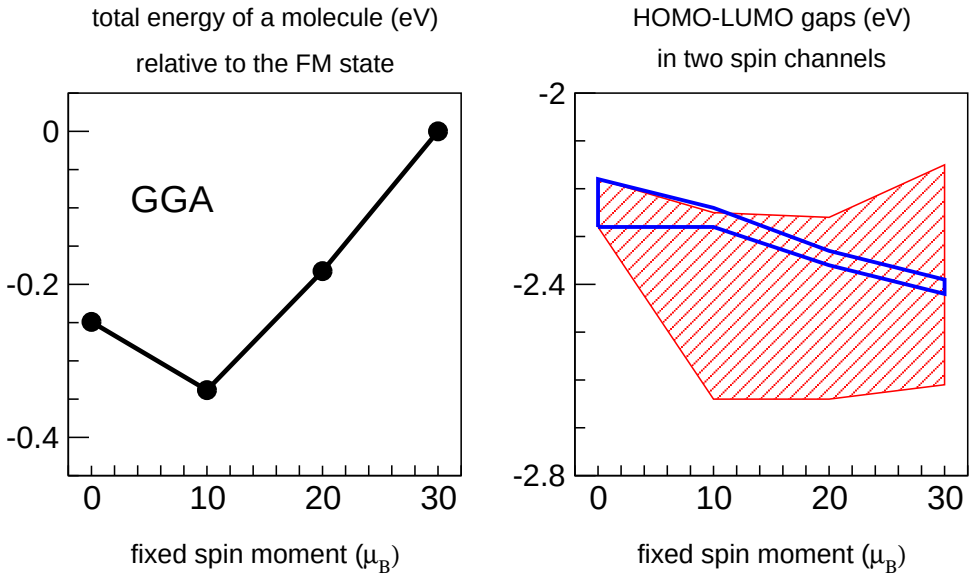

Fig. 4: *Total energy per Fe atom (left panel) and energy gap in two spin channels (right panel; shaded area – majority-spin, thick lines – minority-spin) from fixed spin moment calculations.*

80 K (over both 30→20 and 20→10 μ_B flips). This is qualitatively correct (i.e. indicates a preference toward AFM coupling) and even of the correct order of magnitude. However, two observations can be made here. First, the "true" AFM configuration (with half of magnetic moments inverted on the ring) does not follow the linear trend (see Fig. 4) and lies actually higher in energy than the configuration with two spins inverted. The origin of this is not yet clear to us at the moment. There are several possibilities, the zero-FSM configuration is, technically,the most difficult to converge, so some numerical instability can still play a role. On the other hand, a true (mixed) quantum-mechanical ground state of a system with six coupled S=5/2 spins may win over both our DFT solutions which correspond to selected values S_z=0 or S_z=5 of the total spin. Moreover, the necessity to include magnetic interactions beyond first neighbors, not yet considered at the moment, might further complicate the situation. The second observation concerns the magnitude of exchange parameter J and the fact that it is probably overestimated by a factor of $\sim$4 in our calculation. The origin of this lies most probably in on-site correlations, which, if treated accurately beyond the standard schemes of the DFT, would primarily affect localized Fe$3d$ states, shifting the bulk of occupied states downwards in energy, the bulk of unoccupied states upwards, expanding the energy gap, and – whatever scheme to use for estimating exchange parameters – substantially reducing their magnitude. This effect, with respect to Mn_{12}-ac, has been discussed in the previous Section and made obvious from Table 1.

Summarizing our analysis of the electronic structure of Li- and Na-centered "ferric wheels", one can conclude that the *local* magnetic moments on Fe sites seem to be 4 μ_B rather than 5 μ_B as is often assumed. This implies a valence state closer to Fe(II) than to Fe(III), with a substantial covalent part in the Fe–O bonding. The local spin of S=5/2 per iron site consistent with magnetization measurements is however recovered if one takes the magnetization of neighboring atoms into account. The largest moment is on the apical oxygen atom, followed by smaller moments on nitrogen and the bridging oxygen atoms. This picture is well confirmed by a spatial distribution of spin density.

With respect to its magnetic interactions, this system can be mapped reasonably well onto the Heisenberg model; hence we deal with *rigid* magnetic moments which are nevertheless *delocalized* – an interesting counter-example to the common belief that the Heisenberg model primarily applies to localized spins.

4.2 Ni_4

"Ni_4" is a shorthand notation for a molecular crystal $[Mo_{12}O_{30}(\mu_2\text{–}OH)_{10}H_2\{Ni(H_2O)_3\}_4] \cdot 14\ H_2O$, synthesized and characterized by Müller et al. [73]. This material crystallizes in a structure containing two formula units (shown in Fig. 5), related by the 180° rotation around an edge of the Ni_4 tetrahedron. The Ni–Ni distance is 6.6–6.7 Å, and magnetic interactions are mediated by a longer path than in the systems discussed above.

Magnetic properties are due to Ni^{II} ions in the $3d^8$ configuration (s=1); the ground state is antiferromagnetic. An intriguing aspect of this compound is that the measured zero-field magnetic susceptibility can be very well mapped onto the Heisenberg model, whereas the measurements of magnetization cannot. The inclusion of different anisotropy terms in the Heisenberg model in order to improve the description of experiment had only limited success [74]. First-principles calculations have been performed using the SIESTA method in order to access the electronic structure and estimate the magnitudes of magnetic interaction parameters.

Similarly to the case of the "ferric-wheel" system discussed above, the FSM scheme was used for pinning down different spin configurations and comparing their total energies. The local

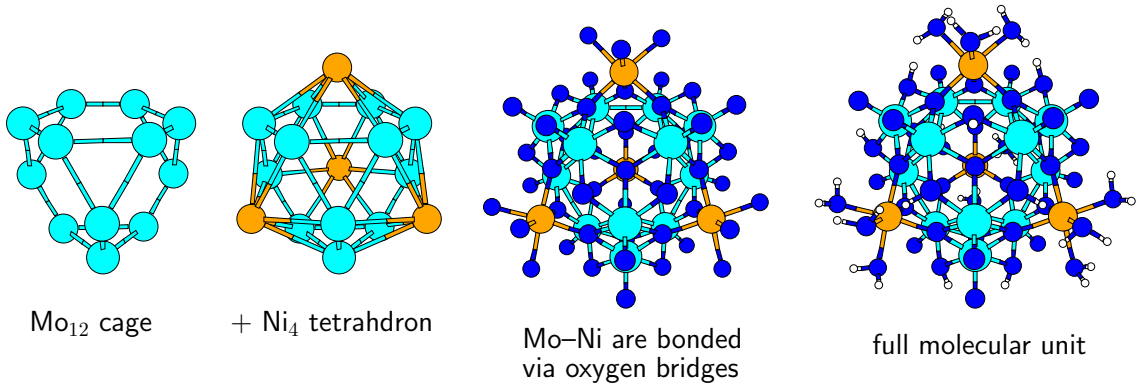

Fig. 5: *Buildup of the "Ni_4" molecular unit.*

DOS is practically indistinguishable for the cases of zero total moment (the AFM structure, which has indeed, in agreement with experiment, the lowest total energy) and configurations with local magnetic moments inverted at one or two Ni atoms (yielding, in the last case, the FM configuration). The local moment per atom in these cases agrees with the s=1 estimation derived from magnetization measurements. As it was discussed above for other magnetic molecules, the magnetic moment is not fully localized on the Ni ion; small but non-negligible magnetization is induced on neighboring oxygen atoms, and even on more distant Mo atoms (Fig. 6, left panel). As the Ni–Ni interaction path is much longer than in other earlier discussed magnetic molecules

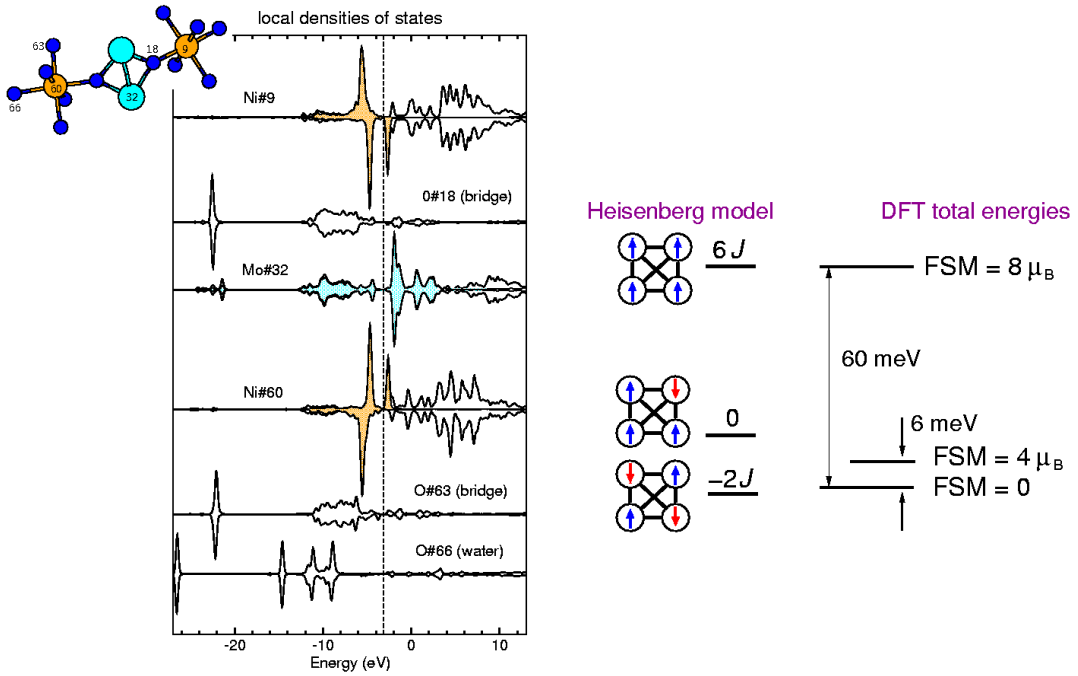

Fig. 6: *Left panel: local DOS of atoms at the Ni–Ni magnetic path. Right panel: a scheme of energy levels in different spin configurations of "Ni_4" according to the Heisenberg model and from first-principles calculations.*

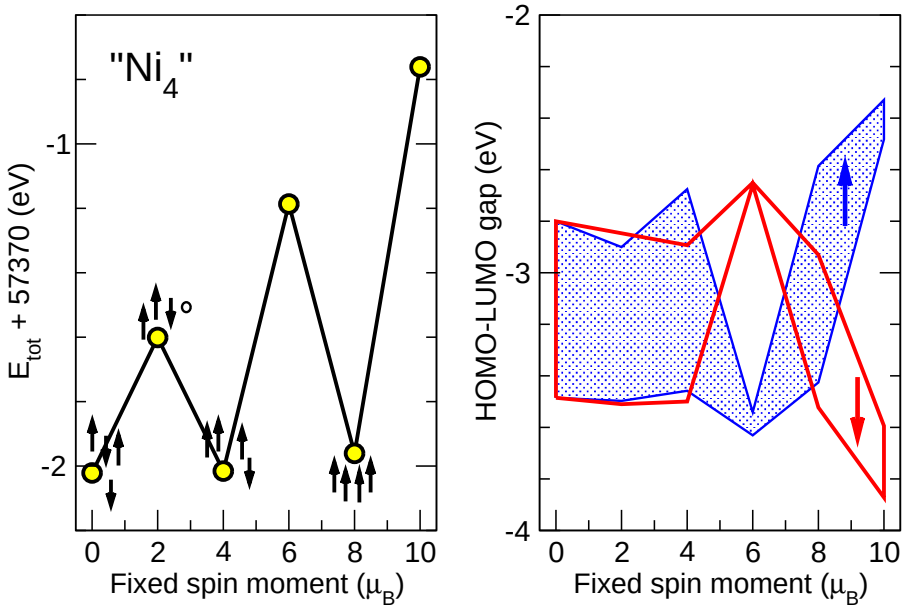

Fig. 7: *Total energy (left panel) and HOMO-LUMO gap (right panel) from FSM calculations of "Ni_4". See text for details.*

(see inset in Fig. 6), the energy differences between configurations with FSM values of 0, 4 and 8 μ_B are small. These solutions are separated by other magnetic configurations which can be converged (2 and 6 μ_B) and correspond to a non-magnetic configuration of one Ni atom, with unchanged and differently coupled s=1 at three others (as schematically shown in Fig. 7, left panel). The energies of these intermediate configurations are substantially higher, and HOMO-LUMO gaps in two spin channels move apart, indicating the necessity of an external magnetic field (hence additional Zeeman energy) for stabilizing these artificial configurations. On the contrary, the three lowest-energy configurations have HOMO-LUMO gaps common for both spin directions (Fig. 7, right panel), therefore the mapping to the Heisenberg model can be done directly, without considering the Zeeman term.

An attempt of such mapping is schematically shown in the right panel of Fig. 6; obviously the sequence of energies of the configurations with one or two spins inverted (starting from the FM solution) is only in qualitative agreement with the Heisenberg model, but the numerical energy differences do not allow for the evaluation of a unique value of J, in contrast to the case of "ferric wheel" discussed above. At best, one can make a rough estimate of the order of magnitude of $-J$, that yields 30 – 90 K. This failure suggests that the magnetic interactions in "Ni_4" are strongly anisotropic, and in any case more sophisticated model Hamiltonian is necessary for its adequate description that the simplest Heisenberg model of Eq. (1).

4.3 A model Fe-binuclear system

Binuclear metal-organic systems form a large, and very simple, group among molecular magnets. Even if their magnetic characteristics like ordering temperature and bulk magnetization are not necessarily outstanding, they help to grasp important physics of $3d$–$3d$ magnetic interaction mediated by an organic ligand and thus offer a convenient model system. Moreover, an interesting effect of spin-crossover has been observed in some such systems, for instance in $[Fe(bt)(NCS)_2]_2$-bpym (bt= 2,2'-bithiazoline, bpym= 2,2'-bipyrimidine): a switch from LS-LS

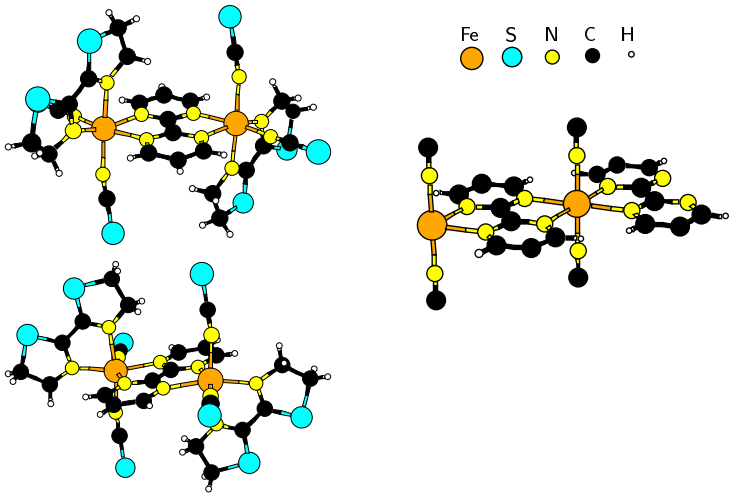

Fig. 8: *Two views of the [Fe(bt)(NCS)$_2$]$_2$-bpym molecule (left panel) and a simplified periodic Fe-binuclear system used in the FLEUR calculation (right panel).*

to LS-HS to HS-HS configuration (LS: low spin; HS: high spin) at the increase of temperature, where the intermediate LS-HS state gets stabilized near 170 K due to an interplay between intermolecular and intramolecular magnetic interactions [75–77]. One demonstrated the possibility of optical switching between different magnetic states and brought into discussion the prospects of their use as active elements in memory devices.

In the present context, such binuclear system will serve as a model molecular magnet, for which we'll assume a simplified structure, but calculate its electronic structure using a method of recognized accuracy, – namely FLEUR code [78], an implementation of the FLAPW method, – with the specific aim to look more precisely at the effect of including intraatomic correlation effects ("Hubbard U"). Starting from the real structure of [Fe(bt)(NCS)$_2$]$_2$-bpym (see Fig. 8, left panel), we "streamline" it somehow to fit it into a compact unit cell for an accurate calculation by a band structure method with periodic boundary conditions (Fig. 8, right panel). This transformation preserved the bipyrimidine part between two Fe centers, but "shortcut" the distant parts of ligands to make a connected structure. One can see that, in contrast to "ferric wheels", the Fe atom is now octahedrally coordinated by nitrogen ions. The resulting partial DOS for self-consistent FM and AFM configurations are shown in Fig. 9. These results have been published in Ref. [79].

Certain similarities can be found with the Fe local DOS in "ferric wheels" – clear splitting into t_{2g}-like and e_g-like states in nearly octahedral ligand field, full occupation of majority-spin Fe$3d$ states and one electron per Fe atom trapped in the Fe$3d$–N$2p$ hybridized band of minority spin. The values of magnetic moments (total per Fe atom in the FM case, along with the local moment, integrated over the muffin-tin sphere) are listed in Table 3. The interatomic exchange parameters have been estimated from total energy differences between FM and AFM cases.

Since the magnetic moment is largely localized at the Fe site, the inclusion of intraatomic correlations beyond the "conventional" DFT might be important. The exchange parameters J depend on the spatial overlap of the d-orbitals on different Fe-sites. It is well known that the d-orbitals within DFT are not localized enough compared to experiment, consequently the J values will be overestimated. There are two main reasons for this shortcoming. First, possible on-site correlations as known from atomic physics are underestimated in case of "conventional" DFT.

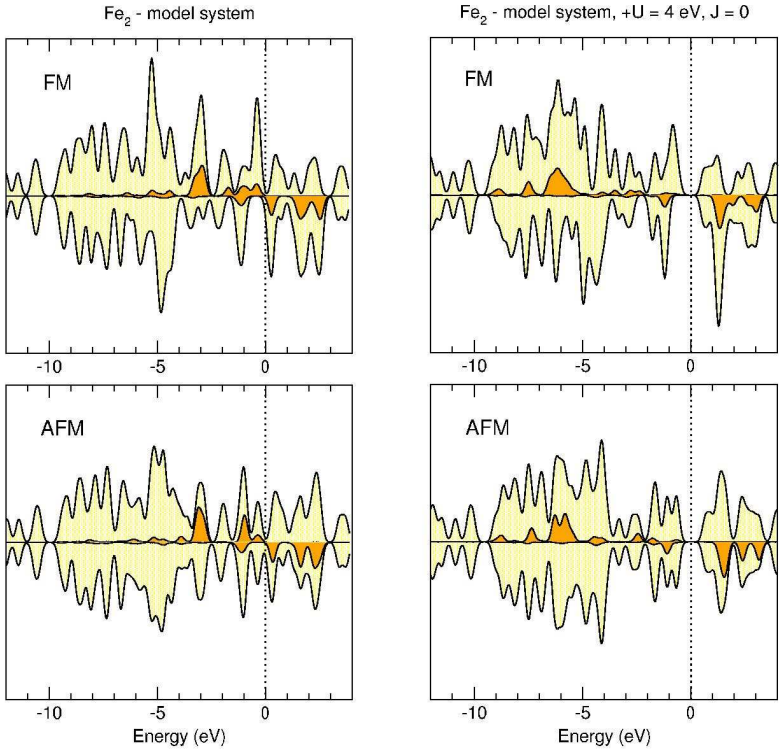

Fig. 9: *Densities of states in FM and AFM cases for the model Fe-binuclear system, calculated by FLEUR in the LDA+U approach. Fe local DOS are shown as shaded areas.*

Second, DFT is not free from spurious self-interactions due to the replacement of the point-like electrons by corresponding densities. Bringing in the atomic physics in the form of LDA+U, i.e., adding a local orbital dependent atomic Coulomb interaction parameter U to DFT [44], would affect the results in the following way: the energies of occupied d-orbitals get lower, whereas the unoccupied ones drift to higher energies. As the energies of spin-flip excitations contribute to the denominator of the nonlocal susceptibility in Eq. (34), this has an effect of reducing the interatomic exchange interaction J. One can recollect that such trend has been already mentioned in relation with the TB-LMTO calculation results of Mn_{12}-ac (Table 1).
The LDA+U scheme leaves it to the user to single out certain orbitals as localized and to choose an appropriate value for the "Hubbard U" parameter. For Fe-binuclear system a presumably reasonable value U=4 eV (based on the experience of other calculations for Fe-based systems)

Table 3: *Magnetic moments and interaction parameters as estimated for a model Fe-binuclear system (Fig. 8) from calculations by FLEUR with and without Hubbard U.*

		M(Fe)	M/Fe	ΔE	J (S=5/2)
U=0	FM	3.62	4.10		
	AFM	3.61	–	102.5 meV	−190 K
U=4 eV	FM	3.93	4.94		
	AFM	3.92	–	76.8 meV	−143 K

has been chosen; in principle, the main motivation here was to study qualitative trends, as we deal with a model system anyway. One observes from Table 3 that the inclusion of intraatomic correlation enhances somehow the local magnetic moment at the Fe site, and to a much smaller extent – the total magnetic moment (in the FM configuration). But the effect on the J parameter much more pronounced; the interatomic magnetic interaction becomes noticeably reduced due to the inclusion of correlation.

4.4 Magnetic anisotropy in single molecule magnets

As a modification of Eq. (3), which introduced the anisotropy in the simplest form, Kortus *et al.* in a number of publications distinguished between axial and transverse anisotropy, with their corresponding parameters D and E, which enter the magnetic spin Hamiltonian (in the second order) as follows:

$$\mathcal{H} = DS_z^2 + E(S_x^2 - S_y^2), \tag{23}$$

The results, both those obtained from calculations with the NRLMOL code and estimated from experiments, are summarized in Table 4 after the data provided by J. Kortus.

Table 4: *Comparison of the calculated by NRLMOL and experimental magnetic anisotropy parameter D for the single molecule magnets. See theory references for computational details.*

Molecule	S	D(K)	
		Theory	Experiment
$Mn_{12}O_{12}(O_2CH)_{16}(H_2O)_4$	10	-0.56^a	-0.56^b
$[Fe_8O_2(OH)_{12}(C_6H_{15}N_3)_6Br_6]^{2+}$	10	-0.53^c	-0.30^d
$[Mn_{10}O_4$(2,2'-biphenoxide)$_4Br_{12}]^{4-}$	13	-0.06^e	-0.05^f
$Co_4(CH_2C_5H_4N)_4(CH_3OH)_4Cl_4$	6	-0.64^g	$-0.7 - -0.9^h$
$Fe_4(OCH_2)_6(C_4H_9ON)_6$	5	-0.56^i	-0.57^j
$Cr[N(Si(CH_3)_3)_2]_3$	3/2	-2.49^i	-2.66^k
$Mn_9O_{34}C_{32}N_3H_{35}$	17/2	-0.33	-0.32^l
$Ni_4O_{16}C_{16}H_{40}$	4	-0.385	-0.40^l
$Mn_4O_3Cl_4(O_2CCH_2CH_3)_3(NC_5H_5)_3$	9/2	-0.58^m	-0.72^n

[a][28], [b][80, 81], [c][82], [d][83], [e][84], [f][85], [g][86], [h][87], [i][88], [j]S. Schromm, O. Waldmann, and P. Müller, [k][89], [l]G. Rajaraman and R. E. P. Winpenny, [m][90], [n][91].

In all the cases presented here the calculated spin ordering is in agreement with experiment. The calculated D parameters for Mn_{12}, Mn_{10}, Mn_9, the ferric star Fe_4 and Cr-amide molecular magnets are in excellent agreement with experimental values. The only remarkable discrepancy is found for Fe_8, a system which seems to pose complications for the DFT treatment. Apparently the DFT may be unable to predict the ground state density accurately enough due to important electronic correlations beyond the mean-field treatment or missing Madelung stabilization (absent in the isolated system).

The SMM listed in Table 4 are in general characterized by a high spin ground-state. However, a high spin state does not necessarily correlate with a high anisotropy barrier. The prefactor D is also very important. In order to increase the barrier one has to understand and control D, which will be the main goal of future research in this area. In all cases where the E parameter is not zero by symmetry it has been predicted with similar accuracy as D – see relevant references for details. The results obtained make one confident in the predictive power of the formalism. It has been already mentioned that a microscopic understanding (based on the electronic structure of SMM) of the magnetic anisotropy parameters is crucial for the rational design of single molecule magnets.

5 Conclusion

Molecular magnetism is a rapidly development topic, and so are first-principles calculations in this domain. Other methods of practical calculation gain recognition beside those chosen for the present outline, and new calculations for different systems appear almost every day. Hopefully this lecture helped to grasp the essential problematics and approaches now in use. In coming years we'll witness the expansion of sophisticated techniques to treat electron correlations, excitation processes and transport properties, well established by now in the study of less complex systems, over the area of molecular magnetism. This might help to resolve several controversies remaining in the present-day interpretation of some materials.

Acknowledgments

The author's research in the field of molecular magnetism became possible within the Priority Program SPP 1137 "Molecular Magnetism" of the Deutsche Forschungsgemeinschaft, the financial support by which is highly appreciated. The work was being done in collaboration with Stefan Blügel, Jürgen Schnack and Manfred Neumann. Many useful discussions with Jens Kortus are appreciated. Parts of the joint review article with Jens Kortus have been used in the preparation of the present manuscript.

Appendix 1. Interatomic magnetic interaction

The following line of argument is due to discussions with V. Anisimov and V. Mazurenko. Given the interaction energy of two quasi-classical spins

$$E = J_{ij}\mathbf{S}_i\mathbf{S}_j\,, \tag{24}$$

its variation due to the change of the angles of the spins $\delta\varphi_i$, $\delta\varphi_j$ reads:

$$\delta^2 E = J_{ij}S^2\delta\varphi_i\delta\varphi_j\,. \tag{25}$$

In the attempt to cast a variation of DFT total energy in a comparable form, one can profit from the Andersen's local force theorem, which works here because we are interested in infinitesimal deviations from the ground state. An explicit derivation of the local force theorem in the desired

form is given in an Appendix of the paper by Liechtenstein et al. [26]. In terms of the Green's function $\mathcal{G}$ and Kohn-Sham Hamiltonian $\mathcal{H}$ the first variation of the total energy reads

$$\delta E = -\frac{1}{\pi}\int^{\epsilon_{\rm F}} d\epsilon \ {\rm Im\,Tr}\left(\delta\mathcal{H}\,\mathcal{G}\right) \tag{26}$$

(which can be shown to be zero), and the second variation

$$\delta^2 E = -\frac{1}{\pi}\int^{\epsilon_{\rm F}} d\epsilon \ {\rm Im\,Tr}\left(\delta^2\mathcal{H}\,\mathcal{G} + \delta\mathcal{H}\,\mathcal{G}\,\delta\mathcal{H}\,\mathcal{G}\right) \ . \tag{27}$$

The variation of the Kohn-Sham Hamiltonian can be explicitly related to rotations in spin space as

$$\delta\mathcal{H} = \frac{i}{2}\delta\varphi_i\left[\mathcal{H},\sigma\right] \ , \tag{28}$$

with the Hamiltonian composed of a spin-dependent part at the site i, with $\Delta_i = V_i^{\uparrow} - V_i^{\downarrow}$ [a potential, in general, non-diagonal in (l,m)] and the rest $\mathcal{H}_0$:

$$\mathcal{H} = \frac{\Delta_i}{2}\begin{pmatrix} 1 & 0 \\ 0 & -1 \end{pmatrix} + \mathcal{H}_0\begin{pmatrix} 1 & 0 \\ 0 & 1 \end{pmatrix} . \tag{29}$$

This yields for the variation of $\mathcal{H}$

$$\delta\mathcal{H} = \frac{i}{2}\delta\varphi_x\ \Delta_i\begin{pmatrix} 0 & 1 \\ -1 & 0 \end{pmatrix} + \frac{1}{2}\delta\varphi_y\ \Delta_i\begin{pmatrix} 0 & 1 \\ 1 & 0 \end{pmatrix} . \tag{30}$$

Extracting from Eq. (27) the terms bilinear in $\delta\varphi_i$, recovering site and spin indexes in the elements of the Green's function G_σ^{ij} and implying the summation in (l,m) yields

$$J_{ij} = -\frac{1}{2\pi}{\rm Im}\int^{\epsilon_F} d\epsilon \left(\Delta_i G_\uparrow^{ij}\Delta_j G_\downarrow^{ji} + \Delta_i G_\downarrow^{ij}\Delta_j G_\uparrow^{ji}\right) . \tag{31}$$

This is the final formula for the interaction between isolated spins in an otherwise infinite and unperturbed environment. If one is interested in the interaction between two *sublattices* of periodically repeated atom types i and j, the Green function follows explicitly in terms of Kohn-Sham eigenfunctions $\psi^{ilm}_{n\mathbf{k}\sigma}$ and eigenvalues $\epsilon_{n\mathbf{k}\sigma}$

$$G^{ij}_{lm,l'm'}(\epsilon) = \sum_{\mathbf{k}n}\frac{\psi^{*ilm}_{n\mathbf{k}}\psi^{jl'm'}_{n\mathbf{k}}}{\epsilon - \epsilon_{n\mathbf{k}}} . \tag{32}$$

Using the following relation for the product of Green's functions

$$\frac{1}{(\epsilon-\epsilon_n)(\epsilon-\epsilon_{n'})} = \frac{1}{\epsilon_n - \epsilon_{n'}}\left(\frac{1}{\epsilon-\epsilon_n} - \frac{1}{\epsilon-\epsilon_{n'}}\right) , \tag{33}$$

the integration in energy over occupied states yields Eq. (17), in terms of a non-local susceptibility, which in a crystal with periodic boundary conditions depends on the Kohn-Sham occupation numbers $n_{n\mathbf{k}\sigma}$,

$$\chi^{ij}_{mm'm''m'''} = \sum_{\mathbf{k}nn'}\frac{n_{n\mathbf{k}\uparrow} - n_{n'\mathbf{k}\downarrow}}{\epsilon_{n\mathbf{k}\uparrow} - \epsilon_{n'\mathbf{k}\downarrow}}\,\psi^{*ilm}_{n\mathbf{k}\uparrow}\psi^{jlm''}_{n\mathbf{k}\uparrow}\,\psi^{ilm'}_{n'\mathbf{k}\downarrow}\psi^{*jlm'''}_{n'\mathbf{k}\downarrow} \ , \tag{34}$$

– a formula probably first given by Liechtenstein et al. [92] and used in a number of publications. It should be understood that this formula implies periodicity and hence describes the interaction between two sublattices rather than two spins. Hence the obtained numbers may be very different from those by straightforward applying of Eq. (17).

Appendix 2. Second-order anisotropy energy

The following derivation of the second-order anisotropy energy, along the lines of Pederson and Khanna [28, 29], has been given by Jens Kortus in Ref. [4]. We proceed from the Cartesian representation of the spin-orbit term

$$U(\mathbf{r},\mathbf{p},\mathbf{S}) = -\frac{1}{2c^2}\mathbf{S}\cdot\mathbf{p}\times\nabla\mathbf{\Phi}(\mathbf{r})\,. \tag{35}$$

Using single-particle wavefunctions expressed in terms of a basis set

$$\psi_{is}(\mathbf{r}) = \sum_{j,\sigma} C^{is}_{j\sigma}\phi_j(\mathbf{r})\chi_\sigma, \tag{36}$$

where the $\phi_j(\mathbf{r})$ are the spatial functions and χ are spin functions, the matrix elements can be expressed as

$$\begin{aligned} U_{j,\sigma,k,\sigma'} &= \langle\phi_j\chi_\sigma \mid U(\mathbf{r},\mathbf{p},\mathbf{S}) \mid \phi_k\chi_{\sigma'}\rangle & (37)\\ &= -i\langle\phi_j \mid V_x \mid \phi_k\rangle\langle\chi_\sigma \mid S_x \mid \chi_{\sigma'}\rangle & (38)\end{aligned}$$

where the operator V_x is defined as

$$\langle\phi_j \mid V_x \mid \phi_k\rangle = \frac{1}{2c^2}\left(\left\langle\frac{d\phi_j}{dz}\middle|\Phi\middle|\frac{d\phi_k}{dy}\right\rangle - \left\langle\frac{d\phi_j}{dy}\middle|\Phi\middle|\frac{d\phi_k}{dz}\right\rangle\right). \tag{39}$$

In the above, $\Phi(\mathbf{r})$ is the Coulomb potential. Thus this treatment uses matrix elements of the Coulomb potential with partial derivatives of the basis functions, thereby avoiding the time consuming task of calculating the gradient of the Coulomb potential directly.
Here we generalize some of the derivations from uniaxial symmetry to an arbitrary one. The same definitions and lettering of the symbols is used as by Pederson and Khanna [29]. In the absence of a magnetic field, the second-order perturbative change to the total energy of a system with arbitrary symmetry can be expressed as

$$\Delta_2 = \sum_{\sigma\sigma'}\sum_{ij} M^{\sigma\sigma'}_{ij} S^{\sigma\sigma'}_i S^{\sigma'\sigma}_j, \tag{40}$$

which is the generalization of Eq. (19) of Ref. [29]. In the above expression, σ sums over the spin degrees of freedom and i,j sums over all the coordinate labels, x,y,z respectively. The matrix elements $S^{\sigma\sigma'}_i = \langle\chi^\sigma|S_i|\chi^{\sigma'}\rangle$ implicitly depend on the axis of quantization. The matrix elements $M^{\sigma\sigma'}_{ij}$ are given by

$$M^{\sigma\sigma'}_{ij} = -\sum_{kl}\frac{\langle\phi_{l\sigma}|V_i|\phi_{k\sigma'}\rangle\langle\phi_{k\sigma'}|V_j|\phi_{l\sigma}\rangle}{\varepsilon_{l\sigma}-\varepsilon_{k\sigma'}}, \tag{41}$$

where $\phi_{l\sigma}$ are occupied and $\phi_{k\sigma'}$ and unoccupied states and ε's are the energy of the corresponding states.
The above equation can be rewritten in a part diagonal in the spin index plus the non-diagonal remainder according to:

$$\Delta_2 = \sum_{ij}\sum_{\sigma} M^{\sigma\sigma}_{ij} S^{\sigma\sigma}_i S^{\sigma\sigma}_j + \sum_{ij}\sum_{\sigma\neq\sigma'} M^{\sigma\sigma'}_{ij} S^{\sigma\sigma'}_i S^{\sigma'\sigma}_j \equiv \boxed{1} + \boxed{2}\,. \tag{42}$$

Using the following relation for the expectation value of a spin operator in a closed shell molecule with excess majority spin electrons ΔN

$$\langle 1|S_i|1\rangle = -\langle 2|S_i|2\rangle = \frac{\langle S_i\rangle}{\Delta N}, \tag{43}$$

the first term of Eq. (42) can be expressed as

$$\boxed{1} = \sum_{ij}(M_{ij}^{11} + M_{ij}^{22})\frac{\langle S_i\rangle\langle S_j\rangle}{(\Delta N)^2}. \tag{44}$$

With the help of

$$\begin{aligned}\langle 1|S_i|2\rangle\langle 2|S_j|1\rangle &= \langle 1|S_iS_j|1\rangle - \langle 1|S_i|1\rangle\langle 1|S_j|1\rangle \\ &= \langle 1|S_iS_j|1\rangle - \frac{\langle S_i\rangle\langle S_j\rangle}{(\Delta N)^2},\end{aligned} \tag{45}$$

and similar relation for $\langle 2|S_i|1\rangle\langle 1|S_j|2\rangle$, and a bit of algebra the second term of Eq. (42) becomes

$$\boxed{2} = \sum_{ij} -(M_{ij}^{12} + M_{ij}^{21})\frac{\langle S_i\rangle\langle S_j\rangle}{(\Delta N)^2} + \frac{1}{4}\sum_i M_{ii}^{12} + M_{ii}^{21}\ . \tag{46}$$

Constructed from Eq.(44) and Eq.(46), the resulting second order shift Δ_2 of Eq. (42) yields Eq. (18). As can be easily verified, for uniaxial symmetry this equation is identical with Eq. (21) of Ref. [29], where the Cartesian off-diagonal M_{ij} matrices vanish and $M_{xx}^{\sigma\sigma'} = M_{yy}^{\sigma\sigma'}$. The above derivation of Eq. (18) did not assume any particular symmetry and is therefore quite general.

References

[1] T. Lis, Acta Crystallogr. Soc. B **36**, 2042 (1980).

[2] O. Kahn, *Molecular Magnetism* (John Wiley & Sons, Singapore, 1993).

[3] W. Linert and M. Verdaguer, eds., *Molecular Magnets* (Springer-Verlag, Wien, 2003), special Edition of Monatshefte für Chemie/Chemical Monthly, Vol. 134, No. 2.

[4] A. V. Postnikov, J. Kortus, and M. R. Pederson, *Density functional studies of molecular magnets*, Scientific Highlight of the month February 2004, Newsletter 61 of the Ψ_k-Network (2004), `http://psi-k.dl.ac.uk/newsletters/News_61/Highlight_61.pdf`.

[5] J. Kortus and A. V. Postnikov, in *Handbook of Theoretical and Computational Nanotechnology*, edited by M. Rieth and W. Schommers (American Scientific Publishers, 2004), vol. 10 of *Encyclopedia of Nanoscience and Nanotechnology*, (in press).

[6] L. Onsager, Phys. Rev. **65**, 117 (1944).

[7] I. Dzyaloshinsky, Journal of Physics and Chemistry of Solids **4**, 241 (1958).

[8] T. Moriya, Phys. Rev. **120**, 91 (1960).

[9] P. W. Anderson, in *Solid State Physics*, edited by F. Seitz and D. Turnbull (Academic Press, New York and London, 1963), vol. 14 of *Advances in Research and Applications*, p. 99.

[10] S. Blundell, *Magnetism in Condensed Matter*, Oxford master series in condensed matter physics (Oxford University Press, 2001).

[11] C. Zener, Phys. Rev. **82**, 403 (1951).

[12] P. W. Anderson and H. Hasegawa, Phys. Rev. **100**, 675 (1955).

[13] P. W. Anderson, Phys. Rev. **115**, 2 (1959).

[14] J. B. Goodenough, Phys. Rev. **100**, 564 (1955).

[15] J. B. Goodenough, J. Phys. Chem. Solids **6**, 287 (1958).

[16] J. Kanamori, J. Phys. Chem. Solids **10**, 87 (1959).

[17] R. M. Dreizler and E. K. U. Gross, *Density Functional Theory. An Approach to the Quantum Many-Body Problem* (Springer-Verlag, Berlin-Heidelberg-New York, 1990).

[18] H. Eschrig, *The Fundamentals of Density Functional Theory*, vol. 32 of *Teubner-Texte zur Physik* (B. G. Teubner Verlagsgesellschaft, Stuttgart – Leipzig, 1996).

[19] W. Kohn and L. J. Sham, Phys. Rev. **140**, A1133 (1965).

[20] K. Schwarz and P. Mohn, J. Phys. F: Metal Phys. **14**, L129 (1984).

[21] V. A. Gubanov and D. E. Ellis, Phys. Rev. Lett. **44**, 1633 (1980).

[22] Z. Zeng, D. Guenzburger, and D. E. Ellis, Phys. Rev. B **59**, 6927 (1999).

[23] L. M. Sandratskii, Adv. Phys. **47**, 91 (1998).

[24] T. Oguchi, K. Terakura, and A. R. Williams, Phys. Rev. B **28**, 6443 (1983).

[25] A. I. Liechtenstein, M. I. Katsnelson, and V. A. Gubanov, J. Phys. F: Metal Phys. **14**, L125 (1984).

[26] A. I. Liechtenstein, M. I. Katsnelson, V. P. Antropov, and V. A. Gubanov, J. Magn. Magnet. Mater. **67**, 65 (1987).

[27] V. P. Antropov, M. I. Katsnelson, and A. I. Liechtenstein, Physica B **237–238**, 336 (1997).

[28] M. R. Pederson and S. N. Khanna, Phys. Rev. B **59**, 693 (R) (1999).

[29] M. R. Pederson and S. N. Khanna, Phys. Rev. B **60**, 9566 (1999).

[30] D. J. Singh, *Planewaves, pseudopotentials and the LAPW method* (Kluwer Academic Publishers, Boston, 1994).

[31] T. Helgaker and P. R. Taylor, in *Modern Electronic Structure Theory, Part II*, edited by D. R. Yarkony (World Scientific, Singapore – New Jersey – London – Hong Kong, 1995), vol. 2 of *Advanced Series in Physical Chemistry*, chap. 12, pp. 725–856.

[32] T. A. Arias, Rev. Mod. Phys. **71**, 267 (1999).

[33] T. L. Beck, Rev. Mod. Phys. **72**, 1041 (2000).

[34] H. Bachau, E. Cormier, P. Decleva, J. E. Hansen, and F. Martín, Rep. Progr. Phys. **64**, 1815 (2001).

[35] J. E. Pask, B. M. Klein, C. Y. Fong, and P. A. Sterne, Phys. Rev. B **59**, 12352 (1999).

[36] P. Blaha, K. Schwarz, G. K. H. Madsen, D. Kvasnicka, and J. Luitz, *WIEN2k, Vienna University of Technology* (2001), improved and updated Unix version of the original copyrighted WIEN-code, which was published by P. Blaha, K. Schwarz, P. Sorantin, and S. B. Trickey, in Comput. Phys. Commun. 59, 339 (1990), `http://url.wien2k.at`.

[37] P. E. Blöchl, Phys. Rev. B **50**, 17953 (1994).

[38] G. Kresse and D. Joubert, Phys. Rev. B **59**, 1758 (1999).

[39] O. K. Andersen, O. Jepsen, and M. Sob, in *Electronic Band Structure and Its Applications: Proceedings, Kanpur, India 1986*, edited by M. Yussouff (Springer-Verlag, Berlin–Heidelberg–New York, 1987), vol. 283 of *Lecture Notes in Physics*, pp. 1–57.

[40] TBLMTO homepage, `http://www.mpi-stuttgart.mpg.de/andersen/`.

[41] O. K. Andersen and O. Jepsen, Phys. Rev. Lett. **53**, 2571 (1984).

[42] D. W. Boukhvalov, A. I. Lichtenstein, V. V. Dobrovitski, M. I. Katsnelson, B. N. Harmon, V. V. Mazurenko, and V. I. Anisimov, Phys. Rev. B **65**, 184435 (2002).

[43] D. W. Boukhvalov, E. Z. Kurmaev, A. Moewes, D. A. Zatsepin, V. M. Cherkashenko, S. N. Nemnonov, L. D. Finkelstein, Y. M. Yarmoshenko, M. Neumann, V. V. Dobrovitski, et al., Phys. Rev. B **67**, 134408 (2003).

[44] V. I. Anisimov, F. Aryasetiawan, and A. I. Lichtenstein, J. Phys.: Condens. Matter **9**, 767 (1997).

[45] M. R. Pederson and K. A. Jackson, Phys. Rev. B **41**, 7453 (1990).

[46] K. A. Jackson and M. R. Pederson, Phys. Rev. B **42**, 3276 (1990).

[47] NRLMOL homepage, `http://cst-www.nrl.navy.mil/~nrlmol`.

[48] M. R. Pederson and C. C. Lin, Phys. Rev. B **35**, 2273 (1987).

[49] M. R. Pederson, B. M. Klein, and J. Q. Broughton, Phys. Rev. B **38**, 3825 (1988).

[50] D. Porezag and M. R. Pederson, Phys. Rev. A **60**, 2840 (1999).

[51] M. R. Pederson, D. V. Porezag, J. Kortus, and D. C. Patton, phys. stat. sol. (b) **217**, 197 (2000).

[52] G. S. Painter and D. E. Ellis, Phys. Rev. B **1**, 4747 (1970), (reference Nr 1 for the DVM method).

[53] A. Rosen, D. E. Ellis, H. Adachi, and F. W. Averill, Journal of Chemical Physics **65**, 3629 (1976), (reference Nr 2 for the DVM method).

[54] Z. Zeng, Y. Duan, and D. Guenzburger, Phys. Rev. B **55**, 12522 (1997).

[55] K. Park, M. R. Pederson, and C. S. Hellberg, Phys. Rev. B **69**, 014416 (2003).

[56] J. M. Soler, E. Artacho, J. D. Gale, A. García, J. Junquera, P. Ordejón, and D. Sánchez-Portal, J. Phys.: Condens. Matter **14**, 2745 (2002).

[57] SIESTA homepage, `http://www.uam.es/siesta`.

[58] P. Ordejón, Computational Materials Science **12**, 157 (1998).

[59] D. Sánchez-Portal, P. Ordejón, E. Artacho, and J. M. Soler, Int. J. Quant. Chem. **65**, 453 (1997).

[60] D. Sánchez-Portal, E. Artacho, and J. M. Soler, J. Phys.: Condens. Matter **8**, 3859 (1996).

[61] J. Junquera, Ó. Paz, D. Sánchez-Portal, and E. Artacho, Phys. Rev. B **64**, 235111 (2001).

[62] R. W. Saalfrank, I. Bernt, E. Uller, and F. Hampel, Angewandte Chemie – International Edition **36**, 2482 (1997).

[63] J. van Slageren, R. Sessoli, D. Gatteschi, A. A. Smith, M. Helliwell, R. E. P. Winpenny, A. Cornia, A.-L. Barra, A. G. M. Jansen, E. Rentschler, et al., Chem. - Eur. J. **8**, 277 (2002).

[64] E. Rentschler, D. Gatteschi, A. Cornia, A. C. Fabretti, A.-L. Barra, O. I. Shchegolikhina, and A. A. Zhdanov, Inorg. Chem. **35**, 4427 (1996).

[65] A. Lascialfari, Z. H. Jang, F. Borsa, D. Gatteschi, A. Cornia, D. Rovai, A. Caneschi, and P. Carretta, Phys. Rev. B **61**, 6839 (2000).

[66] E. K. Brechin, O. Cador, A. Caneschi, C. Cadiou, S. G. Harris, S. Parsons, M. Vonci, and R. E. P. Winpenny, Chem. Commun. **17**, 1860 (2002).

[67] G. L. Abbati, A. Cornia, A. C. Fabretti, A. Caneschi, and D. Gatteschi, Inorg. Chem. **37**, 1430 (1998).

[68] A. L. Dearden, S. Parsons, and R. E. P. Winpenny, Angew. Chem. Int. Ed. Engl. **40**, 151 (2001).

[69] A. V. Postnikov, J. Kortus, and S. Blügel, Molecular Physics Reports **38**, 56 (2003), `http://arXiv.org/abs/cond-mat/0307292`.

[70] O. Waldmann, J. Schülein, R. Koch, P. Müller, I. Bernt, R. W. Saalfrank, H. P. Andres, H. U. Güdel, and P. Allenspach, Inorganic Chemistry **38**, 5879 (1999).

[71] A. V. Postnikov, S. G. Chiuzbăian, M. Neumann, and S. Blügel, J. Phys. Chem. Solids **65**, 813 (2004), `http://arXiv.org/abs/cond-mat/0306430`.

[72] J. P. Perdew, K. Burke, and M. Ernzerhof, Phys. Rev. Lett. **77**, 3865 (1996).

[73] A. Müller, C. Beugholt, P. Kögerler, H. Bögge, S. Bud'ko, and M. Luban, Inorg. Chem. **39**, 5176 (2000).

[74] A. V. Postnikiov, M. Brüger, and J. Schnack, Phase Trans. 2005, to be published); `http://arXiv.org/abs/cond-mat/0404343`.

[75] V. Ksenofontov, A. B. Gaspar, J. A. Real, and P. Gütlich, J. Phys. Chem. **105**, 12266 (2001).

[76] J.-F. Létard, J. A. Real, N. Moliner, A. B. Gaspar, L. Capes, O. Cador, and O. Kahn, J. Am. Chem. Soc. **121**, 10630 (1999).

[77] V. Ksenofontov, H. Spiering, S. Reiman, Y. Garcia, A. B. Gaspar, N. Moliner, J. A. Real, and P. Gütlich, Chemical Physics Letters **348**, 381 (2001).

[78] FLEUR homepage, `http://www.flapw.de`.

[79] A. V. Postnikov, G. Bihlmayer, and S. Blügel, To be published in Computational Material Science (2005), `http://xxx.lanl.gov/abs/cond-mat/0409302`.

[80] K. M. Mertes, Y. Suzuki, M. P. Sarachik, Y. Paltiel, H. Shtrikman, E. Zeldov, E. Rumberger, D. N. Hendrickson, and G. Christou, Phys. Rev. Lett. **87**, 227205 (2001).

[81] A. L. Barra, D. Gatteschi, and R. Sessoli, Phys. Rev. B **56**, 8192 (1997).

[82] J. Kortus, C. S. Hellberg, M. R. Pederson, and S. N. Khanna, Eur. Phys. J. D **16**, 177 (2001).

[83] M. Dressel, B. Gorshunov, K. Rajagopal, S. Vongtragool, and A. A. Mukhin, Phys. Rev. B **67**, 060405 (2003).

[84] J. Kortus, T. Baruah, N. Bernstein, and M. R. Pederson, Phys. Rev. B **66**, 092403 (2002).

[85] A. L. Barra, A. Caneschi, D. Gatteschi, D. P. Goldberg, and R. Sessoli, J. Solid State Chemistry **145**, 484 (1999).

[86] T. Baruah and M. R. Pederson, Chem. Phys. Lett. **360**, 144 (2002).

[87] M. Murrie, S. J. Teat, H. Stockli-Evans, and H. U. Güdel, Angew. Chem., Int. Ed. Engl. **42**, 4653 (2003).

[88] J. Kortus, M. R. Pederson, T. Baruah, N. Bernstein, and C. S. Hellberg, Polyhedron **22**, 1871 (2003).

[89] D. C. Bradley, R. G. Copperthwaite, S. A. Cotton, K. D. Sales, and J. F. Gibson, J. Chem. Soc., Dalton Trans. **1**, 191 (1973).

[90] K. Park, M. R. Pederson, S. L. Richardson, N. Aliaga-Alcalde, and G. Christou, Phys. Rev. B **68**, 020405 (2003).

[91] W. Wernsdorfer, N. Aliaga-Alcalde, D. N. Hendrickson, and G. Christou, Nature **416**, 406 (2002).

[92] A. I. Liechtenstein, V. I. Anisimov, and J. Zaanen, Phys. Rev. B **52**, R5467 (1995).